Transmission Electron Microscopy for Wood and Fiber Analysis − A Review

Mehedi Reza,[a,*] Eero Kontturi,[b] Anna-Stiina Jääskeläinen,[b,c] Tapani Vuorinen,[b] and Janne Ruokolainen [a,*]

This review describes use of transmission electron microscopy (TEM) in wood and fiber analysis. Analytical techniques and sample preparation methods are used to localize substructures of the cell wall polymers and are discussed in this review. The ultrastructural features of the wood cell walls, the structures formed by microfibrils, and the distribution of cell wall polymers, as revealed by TEM, are covered. Research investigating the distribution of lignin in tension and compression woods using TEM is reviewed. Different kinds of wood biodegrading enzymes localized using TEM are mentioned. Additional features of TEM, *i.e.*, 3D imaging, analytical TEM, and electron diffraction are discussed. Lastly, a comparison between TEM and other imaging techniques used for wood and fiber research are made. Thus, this review provides insight into the contribution of TEM in wood research since its invention and demonstrates how to use it more effectively in the future.

Contact information: a: Department of Applied Physics, Aalto University, P.O. Box 11100, FI-00076 Aalto, Finland; b: Department of Forest Products Technology, Aalto University, P.O. Box 16300, FI-00076 Aalto, Finland; c: VTT Technical Research Centre of Finland, Tietotie 2, P.O. Box 1000, Espoo, Finland;
* Corresponding authors: mehedi.reza@aalto.fi; janne.ruokolainen@aalto.fi

INTRODUCTION

Microscopy is the study of fine structures and morphologies using the wide range of microscopy techniques available, which can resolve the details of an object ranging from the millimeter to the sub-nanometer scale. Electron microscopy and its supplementary techniques have been used extensively in most scientific fields. In addition, microscopy has been and is currently being used successfully in wood research to observe wood cells and their sub-cellular components. The invention of the light microscope led to the discovery and description of cells, and it remains influential in wood research. Several sophisticated microscopy and spectroscopy techniques are available, providing high-resolution information about wood cells at the molecular level; *e.g.*, Transmission Electron Microscopy (TEM), Scanning Electron Microscopy (SEM), Atomic Force Microscopy (AFM), X-ray methods, and Raman microspectroscopy are routinely used for wood research (Abe *et al.* 1991; Zimmermann and Sell 2003; Fahlén and Salmén 2005; Peura *et al.* 2008; Gierlinger *et al.* 2010; Raghavan *et al.* 2012; Reza *et al.* 2014b). Bucur (2003) reviewed existing imaging methods for investigating wood structure; however, most of the techniques exhibited low resolution. Nevertheless, transmission electron microscopy, a technique that has been around for approximately 80 years, has one of the highest resolutions (about 0.2 nm for analyzing wood fiber) among

the techniques used in wood and fiber research (Ruska 1934; Duchesne and Daniel 1999). For wood materials, the characteristic dimension of ultrastructural features, which influence the effective material properties, is in the range of few nanometers. Moreover, the formation of three main components (cellulose, hemicelluloses and lignin) and their deposition in the wood cell is still fragmentarily known. Therefore, TEM, a package of 2D imaging, 3D tomography, and elemental analysis with high-resolution, can certainly be used more effectively to understand the sub-cellular structures of wood cells. TEM has already provided invaluable information on ultrastructure of wood cell wall following its development. Meanwhile, TEMs with spherical aberration (C_s) correctors are able to perform imaging with sub-Å resolution (Jiang *et al.* 2012); the performance of such TEM in wood research is, however, limited by the beam sensitivity of the specimens. Cryo-TEMs, a version of TEM, are able to perform imaging of beam-sensitive, low-contrast specimens at liquid N_2 or liquid He temperatures. However, sample preparation and stability under the electron beam have always been challenging steps to overcome for high-resolution imaging of wood specimens at the molecular level. In this review, we have assessed the majority of the information available for TEM analysis of wood materials necessary to overcome complications during analysis. Core areas of evaluation will pertain to the sample preparation, the ultrastructural features of the wood cell wall, and the distribution of cell wall polymers as revealed by TEM. The analytical potential of TEM can essentially be amplified using complementary instruments, and thus these will also be briefly reviewed.

Image Formation in TEM

The basic principles for image formation using TEM are described in Williams and Carter (2009). Briefly, TEM uses an electron beam to image the sample. This provides a higher resolving power than the visible light in optical microscopy. Because the wavelength of the energized electron beam is very short, the diffraction limit is correspondingly lower. Generally, in electron microscopy, high energy primary electrons hit the specimen and the same or different electrons deflect from the sample to form an image. In TEM, a stationary primary electron beam is transmitted through the ultrathin specimen and transformed into a non-uniform electron intensity after transmission or scattering by the specimen (Fig. 1).
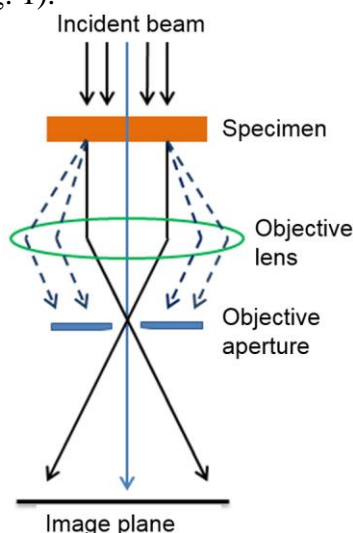

Fig. 1. Schematic diagram showing the mechanism of image formation in bright-field imaging mode in TEM. Dashed lines show the scattered electrons.

bioresources.com

This non-uniform electron intensity hits the fluorescent screen or the electron detector and is translated into image contrast on the screen. Either the direct beam or a diffracted beam is used to form bright-field and dark-field images, respectively. Figure 1 illustrates the mechanism of image formation in the bright-field imaging mode using direct beam. In the bright-field mode, scattered electrons are blocked with an objective aperture in order to enhance the contrast. In addition, while interacting with the specimen, a wide range of secondary signals are produced. Many of them are used in analytical electron microscopy, providing the chemical composition and additional information about the specimens. A TEM analysis must be run under an ultra-high vacuum that prevents scattering of the electron beam by the gas molecules so that the electrons can move freely from the gun through the specimen and further to the detector.

Because of the extraneous materials, low crystallinity, and tight association of cell wall materials it has always been challenging to image the structure and morphology of the wood cell wall. Wood specimens are also more susceptible to radiation damage than the highly crystalline *Valonia*. The direct imaging of cellulose microfibrils in wood using diffraction contrast and low-dose mode has been discussed in Sugiyama *et al.* (1986). A comparison among different cellulose specimens and their sensitivity to the radiation damage at different accelerating voltages is illustrated in Fig. 2. It shows that the radiation damage caused by the energized electron beam can be reduced to an extent using the higher accelerating voltage of the microscope. The unlignified/less-lignified gelatinous layer in tension wood fibers was also found to be a suitable specimen to image with direct beam (Sugiyama *et al.* 1986). The advancement of cryo-TEM also provided the opportunity to image beam sensitive specimens with heavy electron dose. Nowadays, it is possible to keep the specimen temperature below 20 K using liquid helium during the imaging. This way, the electron dose could be increased at least ten times than that at room temperature (Sugiyama *et al.* 1986).
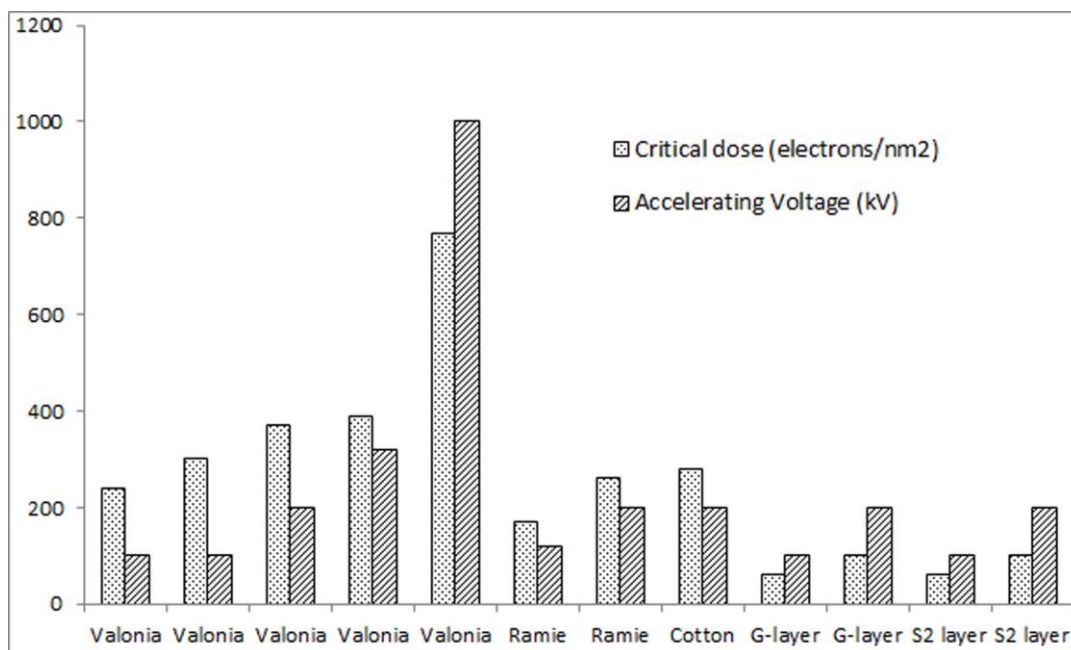

Fig. 2. Accelerating voltage and the corresponding dose at beam damage for different cellulose specimens (Adapted from Sugiyama *et al.* 1986). G-layer: gelatinous layer; S2 layer: middle layer of wood secondary wall.

SAMPLE PREPARATION FOR TEM ANALYSIS

Sample preparation is a very important step because TEM requires ultrathin specimens. Samples for TEM analysis need to be fit on a specimen support known as a grid. TEM grids are metal mesh screens and are about 3 mm in diameter. The size and shape of the mesh vary. They are mainly made of copper, but gold, nickel, and beryllium grids are also used in special circumstances. A fuller discussion on sample preparation protocols for studying cellular ultrastructure of plant tissues with TEM is found in Kuo (2007). In this chapter, essential steps of sample preparation such as replication, sectioning, and staining are discussed.

Replication

The replica technique, an indirect way of looking at specimens, is one of the oldest techniques used in TEM sample preparation. Replicas that have the surface topography of the original specimen can be imaged without exposing beam-sensitive specimens to the electron. This technique was routinely used to study fiber morphology using TEM, especially at the early stage of its invention (Harada 1965). Different types of replication techniques of wood and fiber specimens have been discussed by Côté *et al*. (1964). Briefly, the technique involves the evaporation of a metal or carbon film on the surface of interest, followed by the dissolution of the fiber specimen with an acid (*e.g.,* chromic acid), so that the film is removed. Enhanced contrast can be produced by coating this film with a heavy metal at an oblique angle (20° to 45°). Finally, replicas are collected on the grids for observation (Hafrén *et al.* 2000; Sawyer *et al.* 2008). A TEM surface replica of a kraft pulp fiber is presented in Fig. 3. Hafrén *et al.* (2000) performed platinum replication on the surface of frozen pine wood fractured at -150 °C after being deep etched at an elevated temperature (−95 °C) for 15 min in a freeze-etching apparatus. They obtained a film thickness of 2 nm by high power input for 7 sec. Replication allows for the observation of the lamellar structure of wood cell walls; however, complications in distinguishing between different cell wall layers at a high magnification have been reported (Harada 1965).
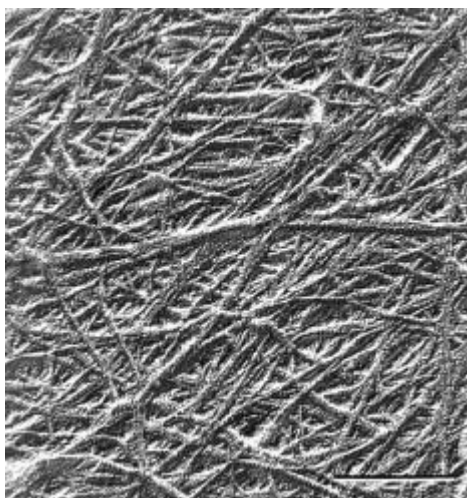

Fig. 3. TEM image of a spruce Kraft pulp fiber surface replica showing the microfibril orientation (Duchesne and Daniel 1999). Scale bar: 100 nm

Sectioning

Specimen thickness is an important factor for imaging with TEM. A thin specimen improves the resolution by reducing image blurring caused by chromatic aberrations. Ultramicrotomy permits the preparation of thin sections to observe the actual structure in a bulk material. A diagram showing the sectioning procedure is presented in Fig. 4. For sectioning, an ultra-microtome, equipped with a diamond knife or a glass knife, is normally preferred. An oscillating diamond knife has been developed to reduce the compression of ultrathin sections (Studer and Gnaegi 2000). Before sectioning, samples are normally embedded in resin after being dehydrated in an ascending series (*e.g.* 30%, 50%, 70%, 90%, and 99.9%) of ethanol/acetone (Bland *et al*. 1971; Maurer and Fengel 1990; Kuo 2007); for instance, Spurr low viscosity resin has been used in electron microscopy for many years (Spurr 1969; Brändström *et al*. 2003). The advantages of the resin embedding include: the preservation of the fine structures, aiding of cutting thin sections, ease the picking of the sections on the grids, and reduced drifting during analysis. The embedding resin can also be removed after sectioning if necessary (Capco *et al*. 1984). Resin embedded samples are sectioned in distilled water to achieve flat and straight sections. However, a block of unembedded wood can also be sectioned at cryogenic or room temperature (Reza *et al*. 2014a,b). Cryogenic sectioning of hydrated samples followed by cryo-TEM provides resistance to chemical fixation and structural changes from dehydration. Different cutting parameters, *i.e.*, cutting angle, speed, section thickness, *etc.,* can be varied during sectioning to improve the section quality. Sectioning also depends on the characteristics of the sample under investigation. Oblique sectioning of resin-embedded wood was performed to avoid some implications of sectioning due to misaligned tracheids and wide lumen compared to the thin cell wall (Donaldson and Xu 2005). In addition, oblique sectioning was used to expose a larger microfibril surface to the enzymes, followed by labelling with gold particles to determine the ultrastructural localization of cellulose and xylan in the birch wood (Blanchette *et al*. 1989a). Since wood is an anisotropic, heterogeneous material, sectioning on different wood surfaces (transverse, radial, and tangential) is necessary in order to obtain a realistic image of the specimen.
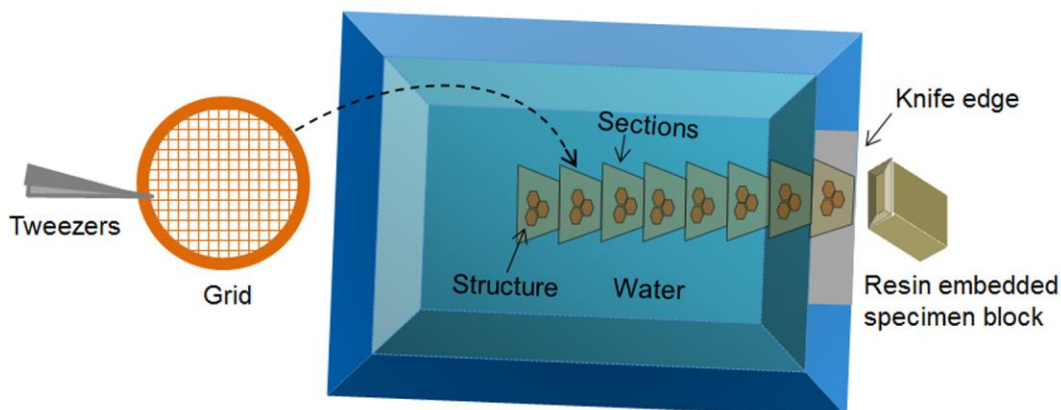

Fig. 4. Schematic diagram of sectioning of a resin embedded specimen block with a diamond knife. A ribbon of sections can be collected onto the grid surface by gently touching (dashed arrow) the sections floating on the water surface. Specimen block must be attached to the microtome arm.

Staining

Staining, an important procedure in specimen preparation, is an auxiliary technique used in microscopy to enhance the contrast of an image by depositing heavy elements onto the specimen. Staining usually enhances the stability of the specimen when visualized with transmitted beam in direct imaging. Sometimes stains can be fixatives, *i.e.*, chemical cross-linkers that cause hardening and increased density. In biology, fixation helps to preserve cells and tissue components in their original state. Staining can be performed before sectioning (pre-staining) or after sectioning (post-staining). Potassium permanganate, osmium tetroxide, and uranyl acetate are the most common stains used in wood research and are discussed below.

Potassium permanganate

Potassium permanganate ($KMnO_4$) is a common stain used for contrasting lignin in wood sections (Bland *et al*. 1971). The stain appears to be specific to lignin, although there are suggestions that it may also stain some hemicelluloses, but not cellulose (Khristova *et al*. 1998). The $KMnO_4$ staining technique was used for studying lignin distribution (Fromm *et al*. 2003; Ma *et al*. 2011a), lignin degradation by rot fungi (Paszczynski *et al*. 1988; Lequart *et al*. 2000), lignification during the cell wall differentiation (Donaldson 1992; Prislan *et al*. 2009), and the properties of pulp fibers (Solala *et al*. 2013).

Bland *et al*. (1971) studied the mechanism of permanganate staining and lignin distribution in the cell wall of the *Pinus radiata*. It was found that the syringyl and guaiacyl groups were mainly responsible for permanganate staining. Experiments with lignin model compounds showed that phenols, especially diphenols and triphenols, rapidly reduced permanganate to manganese oxides (MnO_2) (Bland *et al*. 1971). Perhaps $KMnO_4$ oxidizes the phenolic groups of lignin molecules to aldehydes and carbonic acids. Finally, the resulting water-insoluble MnO_2 is deposited on the section, distinguishing the reaction sites (Koch and Schmitt 2013). According to the degree of lignification, the different cell wall layers exhibit noticeable contrast differences in TEM images after staining with $KMnO_4$ (Fig. 5) (Singh *et al*. 2002a; Lehringer *et al*. 2009; Reza *et al*. 2014a).
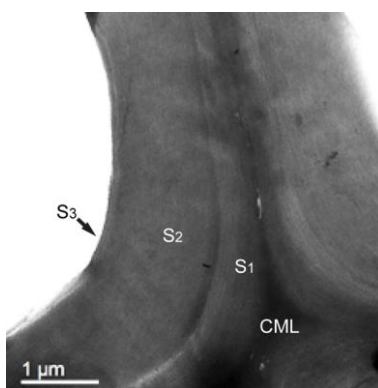

Fig. 5. Micrograph of a $KMnO_4$ stained Norway spruce transverse section through the cell corner taken with a TEM at 80 kV. The compound middle lamellae (CML) region has dark contrast showing the spot of high lignin content. S1, S2, and S3: layers of the secondary wall. Reprinted with permission from Reza *et al.* 2014a. Copyright 2014 American Chemical Society.

The time period for staining the ultrathin sections varied from 2 min to 2 h (Bland *et al*. 1971; Donaldson 2002). The longer the staining time and the higher the $KMnO_4$ concentration, then the probability of contamination with MnO_2 increased (Maurer and Fengel 1990).

In some cases, pre-staining of wood blocks before embedding in resin was preferred to study the ultrastructure of wood (Donaldson 1997; Singh *et al*. 2002a), as post-stained with $KMnO_4$ resulted in contamination of the section surfaces with MnO_2 (Maurer and Fengel 1990). However, this contamination effect was avoided by carefully washing the sections in aqueous citric acid after staining (Greyer 1973). Wood embedded in melamine also had a negligible amount of MnO_2 contamination after staining with $KMnO_4$ (Maurer and Fengel 1990, 1991).

Osmium tetroxide

Osmium tetroxide (OsO_4) is a strong oxidizing agent. It oxidizes many organic materials and becomes reduced to elemental osmium, an easily detectable black substance. As a heavy metal, osmium strongly scatters electrons and is commonly used as a stain and fixative for studying morphology in biological electron microscopy. It is also used for staining polymers when studying their spatial structure using TEM. The OsO_4 compound is a highly volatile and extremely toxic chemical; therefore special care needs to be taken during its handling (Sawyer *et al*. 2008).

Osmium tetroxide is inert towards carbohydrates, but it reacts with unsaturated fatty acids, proteins, and amino acids (Bahr 1954). Although both proteins and unsaturated fatty acids may exist in plant cell walls (Roelofsen *et al*. 1959; Northcote and Lamport 1960), their concentrations are too low to significantly contribute to any reactions with OsO_4. Thus, it has been assumed that the dark contrast regions in the electron micrographs of OsO_4 stained cell walls come from lignin or its precursors (Hepler and Newcombe 1963).

Bland *et al*. (1971) have confirmed that no reactions occur between acetylated lignin and OsO_4. Their results showed the positive reactivity of OsO_4 with double bonds, and di- and trihydroxy phenols. However, compared with $KMnO_4$, OsO_4 only slightly stained the *Pinus radiata* wood sections in the middle lamella region (Bland *et al*. 1971). Fernando and Daniel (2008) used OsO_4 and ruthenium red as pre-staining chemicals, followed by post-staining with $KMnO_4$ to study lignin distribution in the cell wall of pine and spruce thermo-mechanical pulp (TMP) shives. In their study, they observed a highly lignified outer region and a less lignified inner region within the S1 layer of spruce TMP shives, when compared with pine TMP fibers, whereas no variation in electron density was apparent within the S1 layer. Pre-staining with OsO_4 before embedding and post-staining with uranyl acetate and lead citrate was performed to study the protective role of lignin against radiation induced degradation (de Lhoneux *et al*. 1984). Osmium tetroxide has also been used as a pre-staining chemical prior to post-staining with lead citrate to study the ultrastructure of wood (Borgin *et al*. 1975).

Uranyl acetate

Despite its cationic reactivity towards biological materials and acidity in aqueous solution, uranyl acetate has been a widely used negative stain. The main reason for negative staining is to surround the object in a suitable electron-dense material that provides high cellular contrast and good preservation. Uranyl acetate is often the first choice for initial TEM screening of an unknown sample or for rapid preliminary

biological structure quality assessment. The main disadvantage of uranyl acetate for high-resolution studies is the granular/microcrystalline nature of the dried stain and its sensitivity to the electron beam (De Carlo and Harris 2011). The latter can be minimized by the use of low-dose imaging. Basically, the structural detail of the image is limited by the shape and size of the uranyl acetate aggregate as it appears in the projection (Frank 2006).

Uranyl acetate has been mainly used for studying cellulose fibrils (Saito *et al*. 2006) and fines in suspension (Kallavus and Gravitis 1995). Generally, a drop of a dispersion of the sample is mounted on a carbon-coated electron microscope grid. Then, a drop of 1 to 2% uranyl acetate is added before drying. The excess of solution is blotted with filter paper, and the dispersion is dried by natural evaporation (Kallavus and Gravitis 1995; Saito *et al*. 2006).

The combination of uranyl acetate and lead citrate has been successfully used to stain flat sections of non-woody fibers in order to study the distribution of lignin in different cell wall layers (Khalil *et al*. 2006; 2010). Kim *et al*. (2011) stained immunogold labeled sections with uranyl acetate to study xylan and mannan distribution in compression wood. Kallavus and Gravitis (1995) used uranyl acetate staining to study ultrastructural changes in steam exploded wood. These techniques revealed the occurrence of micro-fibrillar bundles in the freshly exploded substrate. The effect of refining and pretreatment on the pulp fibers was also studied by means of this technique (Molin and Daniel 2004; Lei *et al*. 2012).

Immunogold labeling

Immunogold labeling for TEM analysis has played an important role in the fields of cell and tissue biology. This methodology enables precise investigation of the topochemistry of cells and tissues in relation to structural organization. In principle, an antibody localizes and identifies a specific structure in a cell specimen followed by antibody labeling with gold particles (Hayat 2002). The gold particles appear dark in the bright-field image. Using this approach, the distribution of lignin at the ultrastructural level was visualized.

The localization of the dibenzodioxocin structures were studied by counting the number of labeled gold particles in TEM micrographs (Kukkola *et al*. 2003). The dynamics of the deposition of crystalline and amorphous forms of cellulose during cell wall formation have also been studied by TEM and immunogold labeling (Ruel *et al*. 2012). This method was also useful for the investigation of wood degradation by microorganisms (Daniel 1994; Goodell *et al*. 1997).

The progress of lignin deposition and structural variations in the lignin macromolecule during the lignification were studied using immunogold labeling by Joseleau and Ruel (1997) and Ruel *et al*. (1999). The lignin-specific antibodies exhibited no affinity for cellulose and thus provided the necessary sensitivity to detect a discrete amount of lignin by TEM. This technique has been reported as a non-invasive method, which preserves the constituents and the morphology of the material to be studied (Joseleau *et al*. 2004). It also provides more precise and detailed information than the conventional methods, such as lignin stains and autofluorescence (Kukkola *et al*. 2003). Topochemistry of different cell wall polymers studied using this technique is reviewed in the later parts of this paper.

AREAS COVERED BY TEM

Before describing the features of wood ultrastructure and role of TEM, it is important to understand the terminology that will be used. The term "ultrastructure", also known as "fine structure", is used to denote the structural domain of a tissue or cell, as revealed by microscopy, especially electron microscope. The use of ultrastructure in wood science has been intensified after the invention of the electron microscope (Côté 1981). Now the question is "what is the dimension that is considered as ultrastructure?". Precisely, the wood ultrastructure is the hierarchic level ranging from the molecular level up to the cell wall (Eder *et al.* 2013). Thus, the ultrastructure of wood is also reachable with one of the contemporary instruments in light microscope, *e.g.,* the confocal microscope.

Fibrillar Structure of Wood Cell Wall

The basic structure of the wood cell wall has been described in detail in previously reported research (Côté 1964; Daniel 2007). The ultrastructure of the wood cell wall revealed by TEM is the main focus of this paper. Figure 6a illustrates the typical cell wall layering structure, which shows the relative size of each layer and the average microfibril orientation within each layer. This model is acceptable for tracheids; however, there are many deviations from this in ray parenchyma, reaction wood cells, and in normal longitudinal elements (Côté 1981; Alén 2000; Daniel 2007). Transmission electron micrographs of the *Fraxinus mandshurica* cell wall shows two layers (S1 and S2) in the secondary wall (Prodhan *et al*. 1995). The high variability in the thickness of the different wood cell wall layers was shown by TEM investigations (Timell 1973; Singh *et al*. 2002b).
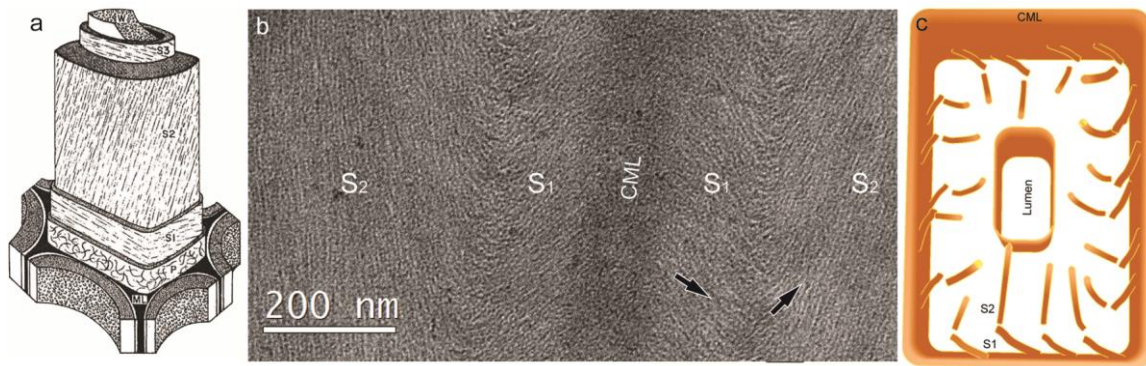

Fig. 6. Schematic diagrams and cryo-TEM image of wood cell walls showing microfibril orientation in different cell wall layers: (a) Model of the wood cell wall with planar microfibril orientation (Côté 1967. Republished with permission of the University of Washington Press); (b) a cryo-TEM image of $KMnO_4$ stained spruce radial longitudinal section showing the microfibril orientation in different layers; and (c) A 3D model based on the high-resolution cryo-TEM where microfibrils form an out-of-plane angle with respect to the cell wall plane. (Figures b and c republished from Reza *et al.* 2014b with permission from Springer-Verlag). ML: middle lamellae; CML: compound middle lamellae; P: primary wall; S1, S2, and S3: layers of the secondary wall; W: warty layer. Arrows show the direction of the microfibril orientation.

The fibrillar structure of the cell wall was confirmed in the early electron microscopic studies of plant materials (Preston *et al*. 1948; Mühlethaler 1949). The

bioresources.com

application of TEM to study the fibrillar structure of wood cell walls in the 1950's provided some details pertaining to the microfibril orientation. Imaging by electron microscopes suggests that microfibrils are synthesized in the plasma membrane by cellulose synthases consisting of a ring of six particles called a rosette (Mueller and Brown 1980; Emons and Mulder 2000). Microfibrils are about 3.5 nm wide (Mühlethaler 1969; Kerr and Goring 1975) and are regularly bridged, forming an interfibrillar bridging element (Donaldson and Singh 1998). Models of microfibrils consisting of 36 and 24 cellulose chains with diamond and rectangular cross-sections were proposed using different analytical techniques, where crystalline chains are surrounded by less crystalline and amorphic chains (Frey-Wyssling and Mühlethaler 1963; Ding and Himmel 2006; Fernandes *et al*. 2011). However, these models were mainly based on indirect evidence and obtained occasionally after removing the associated matrix materials with strong solvents. Since the removal of the surrounding matrix material can change the structure, researchers often prefer microfibrils in a matrix containing fewer non-cellulosic polymers, such as cotton, that possesses a large crystalline dimension. These models are speculations about the true structure of microfibrils in the native wood cell wall.

The presence of granular structures along microfibrils was observed in TEM images of gold-shadowed formvar replicas of tracheid secondary wall (Hodge and Wardrop 1950). Such features were later described as a string of pearls (Manley 1964). The granular structure of microfibrils was also observed in cryo-TEM images of $KMnO_4$ stained spruce wood (Fig. 6b). The explanation behind such structures is unclear in the literature. However, there is evidence that the microfibrils form aggregates in the wood and pulps, as observed by several researchers (Preston *et al*. 1948; Hodge and Wardrop 1950; Hult *et al*. 2003; Reza *et al*. 2014b). These aggregates appear as bundles in the micrograph on the transverse section of the tracheid S2 layer (Singh *et al*. 1998; Singh and Daniel 2001). The aggregation of cellulose microfibrils in wood and pulps controls the accessibility of cellulose (Krässig 1993), thus affecting the extraction of the cell wall components during the biorefinery process; however this mechanism is poorly understood.

The orientation of cellulose microfibrils in woody and non-woody fibers has been revealed by TEM studies. Deposition of microfibrils in lamellae was observed in *Avena coleoptiles* thin sections (Bayley *et al*. 1957) and *Valonia ventricosa* surface replica (Preston *et al*. 1948). Uniform and cross-fibrillar orientations were reported in the secondary wall of *Pseudotsuga taxifolia* wood (Hodge and Wardrop 1950). An S-Z-S helical orientation in the S1, S2, and S3 layers, respectively, was exhibited frequently in models of the wood cell wall (Wardrop 1954; Côté 1981). In the tracheid S1 layer, both S and Z-helical orientations, with an impression of cross-fibrillar structure, were reported (Emerton and Goldsmith 1956; Wardrop 1957; Donaldson and Xu 2005). However, microfibrils perpendicular with respect to the fiber longitudinal axis in single helix have been observed in recent studies (Brändström *et al*. 2003; Reza *et al*. 2014b). The presence of lamellar structure in the S2 layer was proposed based on TEM micrographs of $KMnO_4$ stained softwood sections (Maurer and Fengel 1991; Kerr and Goring 1975), which were interpreted as tangential striations by Chafe (1974). An abrupt change in the orientation of microfibrils between S1 and S2 layers in Norway spruce was observed in TEM images (Brändström *et al*. 2003; Reza *et al*. 2014b), whereas no clear transition was observed between S2 and S3 layers (Donaldson and Xu 2005). In a recent study, Reza *et al*. (2014b) proposed a 3D model of the tracheid wall based on cryo-TEM (Fig. 6b,c) where, in contrast to the existing models of wood cell wall with planar microfibril orientation,

microfibrils protruded from the cell wall plane towards the lumen, forming an out-of-plane angle. Based on the above discussion, it is apparent that the ultrastructure of the wood cell wall is far from being well understood. More systematic studies using high-resolution imaging techniques are required to fully understand the structure of microfibrils and their orientation in native cell walls.

Lignin Distribution

The ultrastructural aspects of cell wall lignification and lignin topochemistry were discussed in detail by Donaldson (2001). In this paper, the focus is on the lignin deposition and topochemistry explored by TEM.

Normal wood

Transmission electron microscopy has been used to obtain high-resolution information about the distribution of lignin in both the developing and the mature xylem (Xu *et al*. 2006a; Ma *et al*. 2011b; Koch and Schmitt 2013). The TEM study on developing tissues in *Pinus thunbergii* showed that the structure of the unlignified middle lamella in the cambium/developing xylem consists of a fine network containing pectin and hemicelluloses (Hafrén *et al*. 2000; Kim *et al*. 2014). As lignification proceeds, the middle lamella becomes compact, dense, and partly covered with globular structures (Hafrén *et al*. 2000). Differences in the temporal synthesis of *p*-hydroxyphenylpropane, guaiacyl, and syringyl units in growing maize internodes were studied by Joseleau and Ruel (1997) using TEM and immunogold labeling. Immunological probes and TEM allowed visualization of the progress of lignin deposition during maturation in each cell type. The TEM images of conifer tracheid cell walls showed an inhomogeneous lignin distribution in the S2 layer after analyzing the electron density variations within the micrographs of $KMnO_4$ stained pine sections (Singh and Daniel 2001; Singh *et al*. 2002a). On the other hand, the TEM micrographs of *Fagus sylvatica* wood sections showed a homogeneous distribution of lignin in the S2 layer (Prislan *et al*. 2009). The distribution of lignin in the ultrathin sections of TMP fibers of rubber wood under high temperatures was examined by Singh and co-workers (2003) using TEM and $KMnO_4$ staining. They also found a heterogeneous lignin distribution in the middle lamella attached to the fiber surface. The degradation/alteration of CML lignin was reported in thermally modified wood (Gao *et al*. 2014). Kukkola and colleagues (2003) localized dibenzodioxocin substructures in lignifying xylem using immunogold labeling and TEM. The abundance of dibenzodioxocin in the softwood lignin was estimated to be approximately 6%, making it one of the major structural units (Ämmälahti *et al*. 1998). Dibenzodioxocin is more abundant in the secondary cell wall layers than in the middle lamella. More specifically, dibenzodioxocin exists in the S2 and S3 layers of secondary cell wall. In young tracheids, where secondary cell wall layers have not appeared yet, the dibenzodioxocin structure was absent (Kukkola *et al*. 2003).

Tension wood

Tension wood is formed in hardwood on the upper side of a leaning stem to maintain the natural vertical orientation of the tree. These fibers are characterized by the formation of an extra layer, termed the gelatinous layer (GL), that may replace part of the secondary cell wall (S1+GL, S1+S2+GL), or occupy the cell lumen attached to the S3 layer (S1+S2+S3+GL), depending on the species and the intensity of the tensile stress (Fig. 7a) (Dadswell and Wardrop 1955; Scurfield 1973; Lehringer *et al*. 2009; Lautner *et*

al. 2012). The GL can be easily separated from the rest of the cell, leaving a fuzzy appearance on the surface of machined wood (Côté *et al*. 1969; Donaldson 2001; Daniel 2007). This layer consists mainly of cellulose microfibrils aligned in the direction of the fiber axis (Lautner *et al*. 2012). The TEM studies on tension wood showed the progression of lignification in the CML, S1, and S2 layers during the GL formation (Yoshinaga *et al*. 2012). Early investigations on the composition of the GL found that it was primarily cellulose (Norberg and Meier 1966) and was entirely free of lignin (Blanchette *et al*. 1994; Wada *et al*. 1995; Donaldson 2001). However, there are a few studies claiming that lignin is present in this layer (Yoshida *et al*. 2002; Joseleau *et al*. 2004). The S1 layer of the gelatinous fiber is less lignified than normal wood (Prodhan *et al*. 1995). Lehringer *et al*. (2009) discovered the deposition of aromatic compounds within the cellulose structure of the GL (Fig. 7a). Non-condensed guaiacyl-syringyl subunits were homogeneously distributed within the S2, S3, and GL, whereas they were absent in the CML (Lehringer *et al*. 2009). A TEM-immunogold study localized condensed guaiacyl structures in the S1 and S2 layers of tension wood fibers. These structures were minimally present in the GL, whereas syringyl units accumulated in the inner GL (Joseleau *et al*. 2004). A low proportion of condensed guaiacyl-syringyl subunits in the S2 region of the fiber walls in *Eucalyptus gunnii* tension wood were reported (Ruel *et al*. 1999). Pilate *et al*. (2004) reviewed the deposition, distribution, and role of lignin in tension wood at the ultrastructural level.
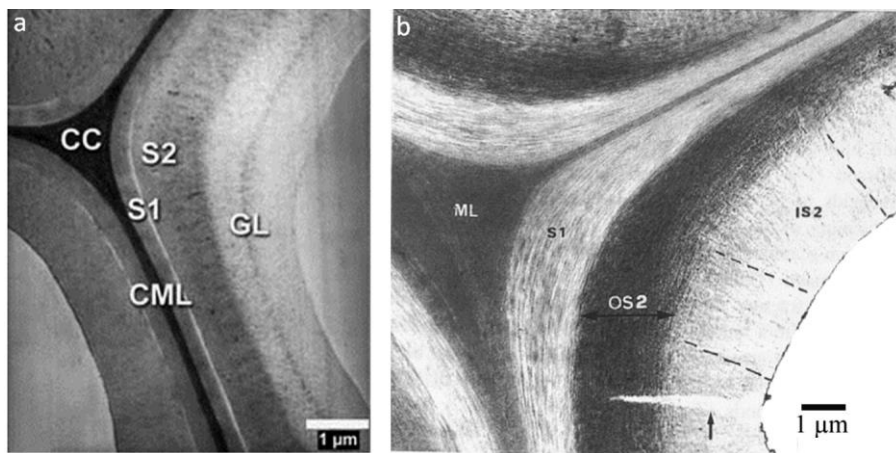

Fig. 7. TEM images of KMnO$_4$ stained resin embedded reaction woods. (a) A maple (*Acer* sp.) tension wood transverse section: the concentric contrast in the gelatinous layer (GL) indicates a slight deposition of aromatic compounds. Figure republished from Lehringer *et al.* 2009 with permission of Springer-Verlag. (b) A compression wood transverse section: outer S2 (OS2) shows dark contrast indicating high lignin content. Arrow shows a characteristic helical check. Figure republished from Singh *et al.* 1998 with permission of author. CC: cell corner; CML: compound middle lamella; ML: middle lamella; S1 and S2: layers of the secondary wall; IS2: inner S2.

Compression wood

Compression wood is formed on the lower side of a branch or on the leaning stem of trees belonging to the orders Coniferales, Ginkgoales, and Taxales (Côté *et al*. 1967). The middle lamella of compression wood is less lignified than normal wood, while the S1 and the inner S2 layers both exhibit a higher lignin concentration than normal wood. The ray cells and the primary cell walls in compression wood have similar chemical

compositions to that of normal wood tracheids (Timell 1982). The deposition of *p*-hydroxyphenyl, guaiacyl, and syringyl in *Pinus thunbergii* compression wood followed the same sequence as in normal wood with some variations (Terashima and Fukushima 1988; Fukushima and Terashima 1991). The TEM image of the compression wood cell wall showed that the outer S2 layer was more lignified than the inner portion, thus stained more intensely with $KMnO_4$ (Fig. 7b) (Singh *et al*. 1998; Kim and Singh 1999; Kim *et al*. 2011). $KMnO_4$ stained compression wood showed higher lignin concentration than normal wood and was more resistant to decay by rot fungi (Blanchette *et al*. 1994).

Distribution of Other Chemical Components

There are many other chemicals that have an important role in the wood cell wall structure. For example, hemicelluloses, one of the matrix materials, play an important role in building the three-dimensional structure of plant cell walls. Combination of TEM and immunogold labeling has proven to be a powerful tool for providing ultrastructural information of hemicellulose distribution in the wood and fiber cell walls. TEM-immunogold labeling of Japanese beech showed the distribution of glucuronoxylans, the main hemicellulosic component of the hardwood, in the secondary wall of xylem cells, but no labelling was found in the primary wall and middle lamella. An even distribution was observed in the inner part of the secondary wall (Awano *et al.* 1998). A uniform distribution of xylan specific antibody was observed in the mature tracheids of Japanese cedar; whereas, glucomannan was distributed in the boundary between the S1 and S2 layers. The innermost part of the cell wall showed stronger labeling with glucomannan than other parts of the cell wall (Kim *et al*. 2010a, b). When applying this technique to pine TMP shives, this yielded information about the distribution of the glucomannan hemicellulose in the different cell wall layers (Fig. 8). Apparently a large number of gold particles were found in the S1 and S2 layers, with less intensity in the primary cell wall. Neither the middle lamella nor the cell corners were labeled (Fernando and Daniel 2008). The localization of glucomannan was studied using immunogold labelling followed by metal replication and was observed with TEM. Glucomannan molecules were distributed heterogeneously all along the cellulose fibril aggregates of Norway spruce kraft pulp. The aggregation of cellulose microfibrils upon the removal of the hemicelluloses was suggested (Duchesne *et al*. 2003). When applying the same technique to developing tension wood in poplar trees, this revealed the presence of xyloglucan in the gelatinous layer (Sandquist *et al*. 2010).

Studies on differentiating normal and compression wood in Japanese cedar revealed the temporal and spatial distribution of xylan and mannan hemicelluloses (Kim *et al*. 2010a, 2011). The xylan specific antibody was uniformly distributed in the S1 layer of compression wood, but it showed an uneven distribution in the S2 layer. Xylan labelling in the inner S2 was mainly detected after beginning of helical cavity in the compression wood; whereas, mannan labelling was detected in the S1 and S2 layer from the early stage of S2 formation (Kim *et al*. 2011). Compared with normal wood, compression wood had significantly different xylan distribution in the secondary wall, but similar mannan labelling (Kim *et al*. 2010a, 2011). The chemical structure of hemicelluloses in wood cell wall may vary depending on the stage of cell wall development (Awano *et al.* 1998; Kim *et al.* 2010b).
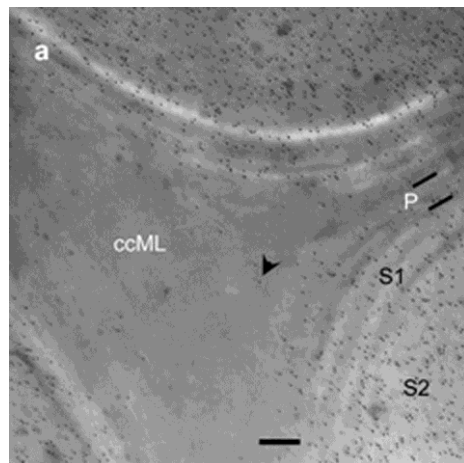
Fig. 8. Immunogold labelling of pine TMP shives showing the distribution of glucomannan in the cell wall. Gradual changes in labeling intensity across the fiber cell wall was apparent; the middle lamella (ccML) is seldom labeled. The primary cell wall (P) has the lowest labeling intensity and the S1 and S2 layers have the highest labeling intensity. Scale bar: 200 nm. Figure republished from Fernando and Daniel 2008 with permission from Authors and Walter de Gruyter.

Hafrén and Westermark (2001) studied the distribution of methylated and acidic pectins in three different wood species using antibody labelling and TEM. In sapwood, pectin was generally present in the highly methyl esterified form, although some acidic pectin was found. In spruce, the methylated form of pectin was more abundant than the acidic pectin. In birch wood, there was a significantly higher amount of methylated pectin than acidic pectin. Also, aspen sapwood contained more methylated pectins than acidic pectins. The degradation of pectic polysaccharides in the CML was reported upon the thermal modification of the wood (Gao *et al.* 2014). The distribution of (1-4)-β-D-galactan in the wood cell wall was studied using different methods, including TEM-immunogold labeling (Altaner *et al.* 2007, 2010; Arend 2008). This carbohydrate epitope is a specific marker of reaction wood within mechanically stressed trees. In compression wood, (1-4)-β-D-galactan was found in the outer cell wall layers and, to a smaller extent, at the interface between the CML and S1 layers (Altaner *et al.* 2007, 2010). In tension wood, (1-4)-β-D-galactan was mainly restricted to the interface between the GL and the adjacent secondary cell wall. It has been suggested that this epitope has a role in cross-linking the secondary wall with the GL (Arend 2008).

Using TEM, Streit and Fengel (1994) studied the distribution of tannin in quebracho heartwood. The results obtained from the lead citrate (stains phenolic extractives selectively) stained sections showed that tannins are located not only in the lumina of vessels, fibers, and parenchyma cells, but also in the cell walls. The formation of tannins and their penetration into the cell wall occurred mainly in a narrow transition zone between the sapwood and heartwood.

Wood Biodegradation

Electron microscopy is a widely used technique for studying the degradation of lignocellulosic material by microorganisms. The decay of wood by basidiomycetes was studied using TEM in Fosiner *et al.* (1985). Daniel (1994) reviewed the use of electron microscopy for aiding the understanding of wood biodegradation. Antibody and immunogold labeling techniques have clearly localized laccase, manganese peroxidase,

lignin peroxidase, and diarylpropane enzymes (ligninase, lignin peroxidase) during the advanced stages of degradation using TEM (Fig. 9) (Blanchette *et al*. 1989b, 1997; Daniel *et al*. 1990, 1991, 2004; Kim *et al*. 1992, 1993; Nicole *et al*. 1992). A TEM study on the degradation of compression wood in a waterlogged condition showed that the initiation of degradation occurred in the inner S2 layer, whereas the outer S2 remained intact (Pedersen *et al*. 2014). Severe bacterial attack was dominant in the secondary wall, and in some cases, bacterial tunneling in the middle lamella of compression wood was also reported (Kim and Singh 1999). Almost similar results were obtained by another study on bacterial decay in pine harbor foundation piles, where TEM was one of the methods used (Rehbein *et al*. 2013). Ray parenchyma and epithelial cells remained unaffected by bacteria because of the high lignin content (Pedersen *et al*. 2014). The TEM imaging showed the colonization of fungal hyphae in the fiber cell lumen of a copper-chromium-phosphorus preservative-impregnated fence pole (Råberg and Daniel 2009). The TEM studies on fiber degradation by rot-fungi showed the presence of fungi in the cell lumen at an early stage of degradation and, at the advanced stage, they appeared to have infiltrated the cell wall structure (Highley *et al*. 1983; Khalili *et al*. 2000). Investigations on the decay of normal and reaction woods showed that compression wood was more resistant to decay than the normal wood, whereas tension wood had similar amounts of decay as normal wood that was caused by white or brown rot fungi. Although the gelatinous layer did appear to be somewhat expanded and swollen, the highly crystalline cellulose remained relatively intact even in the most severely decayed areas of the wood (Blanchette *et al*. 1994).
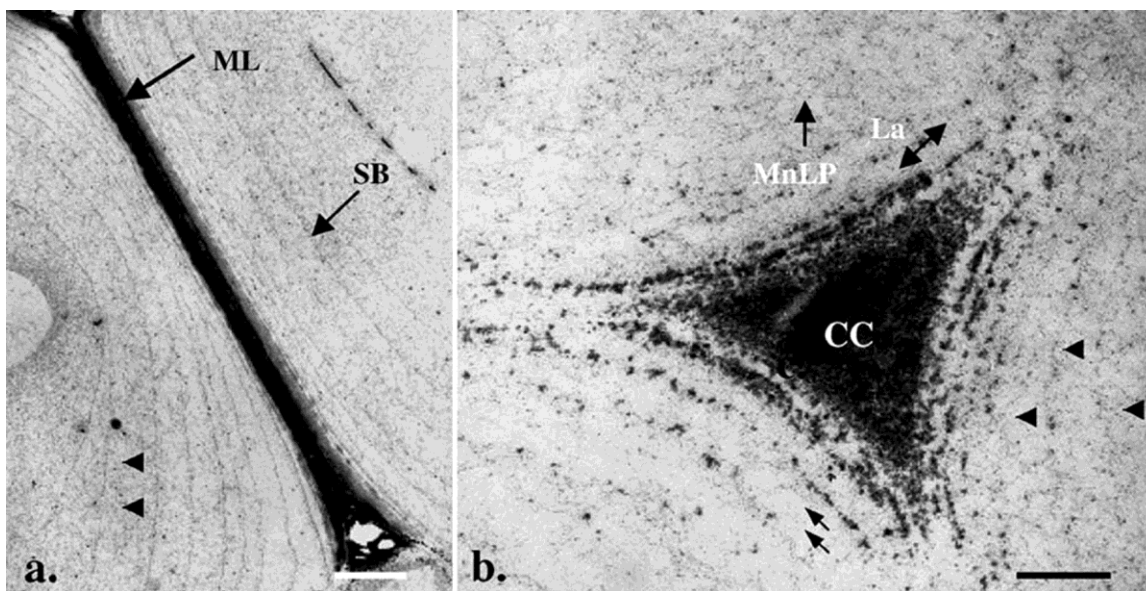

Fig. 9. TEM images showing morphology of birch cell wall decayed by *P. radiata* wild and localization of laccase and MnP/LiP. (a, b) Advance stage of attack with only parts of the S1 and middle lamella region (ML) and cell corners (CC) remaining. Concentric bands (SB) of extracellular slime are arranged in the S2 layer and are apparent between the bands (arrowheads) and between the remaining delaminated S1 layer surrounding the CC (double arrows). Laccase (La), manganese peroxidase (MnP), and lignin peroxidase (LiP) enzymes were found associated with the degraded cell-wall, as well as the extracellular slime material. Reproduced from Daniel *et al.* 2004. Copyright © 2004 Elsevier Masson SAS.

COMPLEMENTARY TECHNIQUES COUPLED WITH TEM

3D Imaging

Electron tomography is a useful technique for revealing 3D information about wood structure, since TEM micrographs provide only 2D projections of the 3D objects. In tomography, a series of images are taken at different tilt angles and reconstructed into a 3D volume.

X-ray tomography on spruce wood has been produced; however, researchers were only able to observe the features with dimensions over 1.5 µm (Trtik *et al*. 2007). In contrast, a TEM having a goniometer with a high enough tilt range (-60° to +60°), can acquire angular increments of about 1° to 3°, thus providing a high-resolution electron tomography. In practice, the tilt range is limited, *i.e.* specimen cannot be tilted ± 90° which degrades the resolution in the *z* direction (parallel to the incident electron beam). However, this problem can be solved by applying dual-axis electron tomography, but the sample may suffer from beam damage because the sample is continuously exposed to the electron beam during the acquisition of tilt series. This problem can be overcome to an extent by using cryo-TEM and the low-dose mode of the automated acquisition software. The reconstruction software can be found online, and the many of the programs are free and user friendly. In practice, further image processing is required to separate individual microfibrils digitally in the tomograms (Ciesielski *et al*. 2013).

Xu *et al*. (2007) performed a dual-axis electron tomography to investigate the 3D organization of cellulose microfibrils in plastic resin-embedded, delignified cell walls of radiata pine early wood. In this study, Xu and colleagues were able to digitally isolate individual microfibrils from associated lignin and hemicelluloses (Fig. 10). They stained the wood sections with several chemicals to enhance contrast and beam stability. Effective use of electron tomography on ultrathin wood sections would help to resolve many of the questions regarding the helical organization of microfibrils in different layers, lamellar (radial/tangential) structure of the S2 layer, and the structure of transition layers. A 2D projection of an anisotropic, heterogeneous material like wood seems to be insufficient.
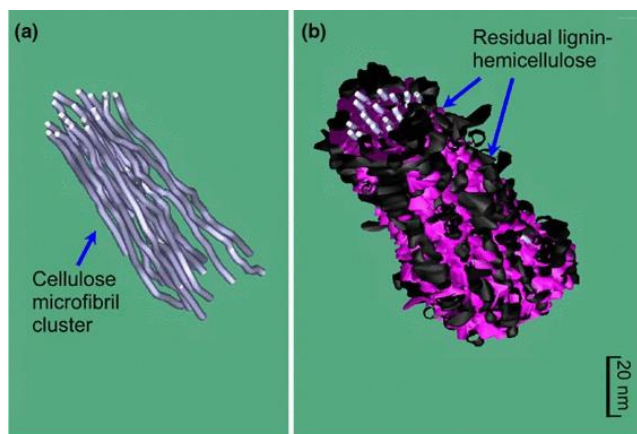

Fig. 10. Models of cellulose microfibril clusters in the radiata pine S2 layer obtained by tracking tomographic slices. (a) Model of a microfibril cluster without associated lignin and hemicelluloses, and (b) model of the same microfibril cluster with residual lignin and hemicelluloses. Figure republished from Xu *et al.* 2007 with permission given by Springer-Verlag.

Analytical TEM

Energy Dispersive X-ray Spectroscopy (EDX or EDS) and Electron Energy-Loss Spectrometry (EELS) are the TEM analytical techniques for the elemental analysis or chemical characterization of specimens. The basic principle of these techniques can be found in Michler (2008) and Williams and Carter (2009). These techniques have been used in wood chemistry. Studies of different hardwood species using TEM-EDX showed higher lignin concentration in the cell corner middle lamella than in the secondary cell wall (Eriksson *et al*. 1988; Xu *et al*. 2006b). The TEM-EDX analysis was used to determine the quantitative distribution of guaiacyl and syringyl units in the cell wall of brominated white birch (Saka and Goring 1988). The distribution of impregnated chemicals within the wood cell wall was also studied using this technique (Wallström and Lindberg 2000). Dünisch *et al*. (1998) determined the potassium (K) and calcium (Ca) concentration in phloem, cambium, and xylem cells of spruce by TEM-EDX during the formation of earlywood and latewood. During cell enlargement, a strong increase of the K content was detected. An increase of the Ca content of differentiating cells was found during secondary wall formation, whereas the Ca content of the cell wall decreased remarkably during its lignification.

Localization and characterization of manganese species during the graft copolymerization of acrylic acid onto sawdust was performed by TEM and EELS using $KMnO_4$ as an initiator. The results obtained by EELS showed that MnO_2 deposited on wood participates in the grafting mechanism of acrylic acid (Marchetti *et al*. 2000). The high-resolution examination of the distribution of a partially methylated hydroxymethyl melamine resin in Norway spruce earlywood cell walls was performed using this technique (Rapp *et al*. 1999). The nitrogen in the resin produced detectable signals in all the layers of the lignified cell walls, thus allowing for the quantification of resin that had penetrated into the different layers. However, the application of these analytical techniques in wood samples would be limited by the rapid degradation by the electron beam.

Electron Diffraction

The crystal is a set of lattice planes that reflects radiation according to Bragg's law ($2d\ sin\ \theta = \lambda$; where the periodicity is d, the diffraction angle is 2θ, and the wavelength is λ). In TEM, the wavelength of the electron is very small; therefore the lattice planes will diffract electron when they are almost parallel to the incident beam (Sawyer *et al*. 2008). Electron diffraction has proven to be a powerful tool for providing ultrastructural information of cellulose microfibrils originating from different sources (Fig. 11) (Preston and Ripley 1954). However, the use of electron diffraction in native wood is limited because of the presence of both crystalline and amorphous materials in wood. An unoriented amorphous material gives a diffraction pattern consisting of broad rings, which poses difficulty to extract diffraction of the crystalline structure. Therefore, delignification of wood specimen is usually performed before extracting a diffraction pattern of crystalline cellulose in wood cell wall (Adachi *et al*. 1991). Microfibrils in a matrix containing fewer non-cellulosic polymers, such as *Valonia*, are often preferred to acquire diffraction (Preston and Ripley 1954). The unlignified/less-lignified gelatinous layer in tension wood fibers was also found to be a suitable specimen for TEM analysis (Sugiyama *et al.* 1986). Furthermore, wood specimens are susceptible to radiation damage during the acquisition of diffraction pattern. In the case of cellulose, it was reported that the radiation damage results in an increase of d spacing with increasing

irradiation doses (Revol 1985). This can be a probable reason for incompatibility between the results obtained with electron and X-ray diffraction (Sugiyama *et al.* 1991b; Nishiyama *et al.* 2002). However, specimen damage can be reduced to an extent using low-dose imaging mode and with one of the contemporary cryo-TEM. Electron diffraction on the algal cell wall showed the co-existence of both I_α and I_β polymorphs with variable proportions (Sugiyama *et al.* 1991a, b). These polymorphs have closely related molecular conformation, but they have different hydrogen bonding patterns. In higher plants, cellulose I_β is thought to be the dominant polymorph (O'Sullivan 1997).
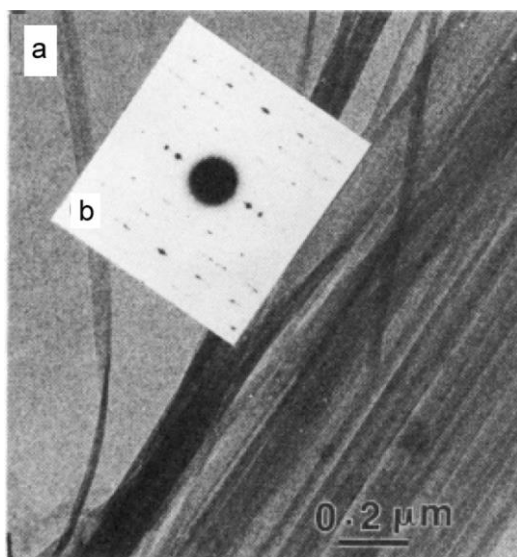

Fig. 11. Ultrastructural features of *Microdictyon* alga cellulose microfibrils: (a) a thin layer of unstained microfibrils observed under low-dose imaging condition; and (b) electron diffraction collected from an area such as that located in the lower part of "a". Adapted with permission from Sugiyama *et al.* 1991b. Copyright 1991 American Chemical Society.

TEM VERSUS OTHER TECHNIQUES

The invention of TEM in 1940s brought in a new era for the wood scientists and has continued to generate significant contribution to the field. Later, the development of replication, ultramicrotomy, and embedding in resin added the flexibility of studying small specimens extracted from a whole tree. The combined effort of these techniques generated information on wood ultrastructural already in 1950s (Wardrop 1954). The application of electron diffraction on algal cellulose microfibrils provided details of cellulose polymorphism and crystal structure (Preston and Ripley 1954; Sugiyama *et al.* 1991a, b). Electron tomography has been available for over 30 years and has been a useful technique for exploring 3D biological structures. However, the application of this technique in wood research has started from last decade (Xu *et al.* 2007). In a recent study, Ciesielski and co-workers (2013) visualized individual microfibrils in pretreated plant cell walls using electron tomography and computational analysis. The development of energy-filters and corresponding instruments has enabled energy-filtered TEM (EFTEM) which is a useful technique for two- and three-dimensional imaging, and chemical analysis at the nanometer scale. An example of zero-loss imaging with a cryo-TEM equipped with an Omega type energy filter is available in Reza *et al.* (2014b).

bioresources.com

Following its invention, the addition of new features and instruments has made TEM one of the leading techniques in biology and material science. Likewise, TEM has provided a solid foundation in the visualization and discovery into the wood cell wall structure and will continue to be a major instrument in wood research for years to come. Although TEM has some issues regarding the preparation of ultrathin specimens, the resolving power of TEM is reported to be higher than other available techniques for wood and fiber specimens (Duchesne and Daniel 1999). Electron beam irradiation is one of the major limiting factors of reaching high-resolution with electron microscopy. This can be reduced to a tolerable level by using cryo-TEM and low-dose imaging mode. The use of cryo-sectioning followed by cryo-TEM imaging allows for the investigation of hydrated specimens without any structural collapse. However, there are many other techniques that have been used to study wood structure independently. The limitations of TEM could be minimized by choosing one of those techniques as a complement. Table 1 summarizes the opportunities and challenges of principal imaging techniques used in wood research.

It is also possible to study hydrated specimens in environmental scanning electron microscope (ESEM) and low-vacuum scanning electron microscopes (LVSEM). Scanning electron microscopy has a large depth of field, which produces a 3D-like image of the specimen surface (*e.g.* micrographs of compression wood in Burgert *et al*. 2004); whereas, in TEM, the image is a 2D projection of the specimen, independent of the topography, as long as it is transparent to the electron beam. Scanning electron microscopy, with focused ion beam technology (FIB-SEM), allows 3D imaging of a volume of interest in the specimen block. However, prolonged exposure to the electron beam can cause significant artefacts. Furthermore, the 3D FIB-SEM is still in a developing stage and requires significant upgrading of hardware (beam stability and detector performance), software (automated), sample preparation technique, and data processing and interpretation (Bassim *et al*. 2014). Like TEM, SEM with EDX technology can be used to perform elemental analysis of the wood specimens (Westermark *et al*. 1988). Field emission SEM (FESEM) has been successfully used to study the microfibril orientation in wood cell walls (Abe *et al*. 1991).

X-rays are one of the oldest techniques used to study wood structure. High-resolution information about the average microfibril orientation in the wood cell wall can be found in Farber *et al*. (2001). Using synchrotron X-ray microdiffraction, the helical organization of microfibrils in the spruce S2 layer was studied (Lichtenegger *et al*. 1999). Studies on algae and wood cell walls with X-ray diffraction showed the crystalline structure of cellulose microfibrils with atomic resolution (Nishiyama *et al*. 2002; Fernandes *et al*. 2011). Three-dimensional tomography was also performed using this technique with very low-resolution (Trtik *et al*. 2007). Depending on the size of the beam in Small Angle X-ray Scattering (SAXS), it is possible to either scan the sample with spatial resolution down to the μm-range or to obtain an average information over a larger sample volume containing many cells. However, this method cannot distinguish between two cell types with different microfibril angles (MFA), or even one cell type showing two MFAs; therefore, the benefit of averaging over several cells requires some previous knowledge about the system. In addition, issues regarding radiation damage were reported while analyzing wood specimens (Saxe *et al*. 2014).

Atomic force microscopy (AFM) has been used as an important complement to electron microscopy to study the wood ultrastructure for a prolonged duration (Fahlén and Salmén 2005; Zimmermann *et al*. 2006). However, there are issues limiting high-resolution imaging due to the finite size of the AFM tip, which exaggerates the size of

very small (<50 nm) features (Duchesne and Daniel 1999). Besides imaging, AFM can be used to study the micro-mechanics of the wood cell wall using the nano-indentation method (Burgert and Keplinger 2013).

Raman microspectroscopy has been considered as a non-destructive technique to study the distribution and orientation of wood cell wall materials (Gierlinger *et al*. 2010; Hänninen *et al*. 2011). Nevertheless, the mapping of specimens can be disturbed by laser induced damage and excess fluorescence (Gierlinger *et al*. 2012).

Table 1. Principal Imaging Methods Used in Wood Research with their Features and Challenges

Techniques	Opportunities	Challenges
Transmission Electron Microscopy (TEM)	Imaging, elemental analysis, tomography, diffraction, imaging of hydrated specimen with cryo-TEM; resolution 0.2 nm.	Sample preparation, radiation damage.
Scanning Electron Microscopy (SEM)	High depth of focus, imaging of hydrated specimens with LVSEM and ESEM, elemental analysis with EDX, 3D imaging with FIB-SEM, block of specimen can be imaged; resolution 1.0-10.0 nm depending on the imaging mode.	Radiation damage, charging of non-conductive specimens, all the features may not be available in a single package.
Atomic Force Microscopy (AFM)	Height imaging, phase imaging, studying micro-mechanics with nano-indentation, imaging can be performed at ambient temperature and humid conditions and in fluid environments, easy sample preparation, no need for high vacuum; lateral resolution 2 nm.	Tip-sample interaction can generate artefacts.
Raman Microscopy	Image reconstruction with characteristic band, chemical analysis, spectroscopy, easy sample preparation; resolution <0.5 µm.	Laser induced damage, fluorescence effect during mapping, precise focusing needed in confocal mode.
X-Ray	Diffraction, spectroscopy, tomography, generates average microfibril angle of the analyzed specimen.	Sometimes prior knowledge on the specimen needed; cannot distinguish between two cell types with different structure.

CONCLUSIONS

1. This review demonstrates the importance and potential use of TEM in the investigation of wood and fiber cell wall ultrastructure. Several staining methods are used in TEM. Among these, KMnO4 staining is a common method for studying lignin distribution in wood cell walls. Immunogold labeling requires several preparation steps, but it is an important technique to localize the substructures of cell wall polymers. Negative staining with uranyl acetate has been found suitable for studying cellulose microfibrils and fines.

2. The orientation of microfibrils and the structures formed by microfibrils (*e.g.*, aggregates, bundles) in wood cell walls have been investigated successfully using

TEM. The molecular structure of microfibrils using electron diffraction in the algal cell wall provided some details about cellulose polymorphisms and their existence in the native cell wall.

3. A substantial amount of research has investigated the distribution of lignin using TEM. This technique is also useful in studying specific features of tension and compression woods.

4. The distribution of hemicelluloses in the wood cell wall has been studied successfully using TEM and immunogold labeling. The TEM-immunogold labeling technique has also been used to localize enzymes during advanced stages of degradation.

5. Some additional features of TEM, such as acquiring tilt series, EDX, EELS, and diffraction are promising complementary features which have provided additional information about the wood structure. However, very few studies have been performed using these technologies in wood. Further research should focus on the 3D imaging of wood ultrastructure with improved sample preparation methods.

ACKNOWLEDGEMENT

REFERENCES CITED

Abe, H., Ohtani, J., and Fukazawa, K. (1991). "FE-SEM observations on the microfibrillar orientation in the secondary wall of tracheids," *IAWA J.* 12(4), 431-438. DOI: 10.1163/22941932-90000546

Adachi, H., Sugiyama, J., Kondo, Y., and Okano, T. (1991). "The difference of cellulose crystal between softwoods and hardwoods," *Sen'i Gakkaishi* 47(11), 580-584.

Alén, R. (2000). "Structure and chemical composition of wood," *Forest Product Chemistry (Papermaking Science and Technology, Book 3)*, P. Stenius (ed.), Fapet Oy, Helsinki, Finland.

Altaner, C., Hapca, A. I., Knox, J. P., and Jarvis, M. C. (2007). "Detection of β-1-4-galactan in compression wood of Sitka spruce [*Picea sitchensis* (Bong.) Carrière] by immunofluorescence," *Holzforschung* 61(3), 311-316. DOI: 10.1515/HF.2007.049

Altaner, C. M., Tokareva, E. N., Jarvis, M. C., and Harris, P. J. (2010). "Distribution of (1→4)-β-galactans, arabinogalactan proteins, xylans and (1→3)-β-glucans in tracheid cell walls of softwoods," *Tree Physiol.* 30(6), 782-793. DOI:10.1093/treephys/tpq021

Arend, M. (2008). "Immunolocalization of (1-4)-β-galactan in tension wood fibers of poplar," *Tree Physiol.* 28(8), 1263-1267. DOI: 10.1093/treephys/28.8.1263

Awano, T., Takabe, K., and M. Fujita, M. (1998). "Localization of glucuronoxylans in Japanese beech visualized by immunogold labelling," *Protoplasma* 202, 213-222. DOI: 10.1007/BF01282549

Ämmälahti, E., Brunow, G., Bardet, M., Robert, D., and Kilpeläinen, I. (1998). "Identification of side-chain structures in a poplar lignin using three-dimensional

bioresources.com

HMQC−HOHAHA NMR spectroscopy," *J. Agric. Food Chem.* 46(12), 5113-5117. DOI: 10.1021/jf980249o

Bahr, G. F. (1954). "Osmium tetroxide and ruthenium tetroxide and their reactions with biologically important substances: Electron stains III," *Exp. Cell Res.* 7(2), 457-479. DOI: 10.1016/S0014-4827(54)80091-7

Bassim, N., Scott, K., and Giannuzzi, L. A. (2014). "Recent advances in focused ion beam technology and applications," *MRS Bulletin* 39(4), 317-325. DOI: 10.1557/mrs.2014.52

Bayley, S. T., Colvin, J. R., Cooper, F. P., and Cecily, A. (1957). "The structure of the primary epidermal cell wall of *Avena coleoptiles*," *J. Biophys. Biochem. Cytol.* 3(6), 171-182. DOI: 10.1083/jcb.3.2.171

Blanchette, R. A., Abad, A. R., Cease, K. R., Lovrien, R. E., and Leathers, T. D. (1989a). "Colloidal gold cytochemistry of endo-1,4-β-glucanase, 1,4-β-d-glucan cellobiohydrolase, and endo-1,4-β-xylanase: ultrastructure of sound and decayed birch wood," *Appl. Environ. Microbiol.* 55(9), 2293-2301.

Blanchette, R. A., Abad, A. R., Farrell, R. L., and Leathers, R. L. (1989b). "Detection of lignin peroxidase and xylanase by immunocytochemical labeling in wood decayed by basidiomycetes," *Appl. Environ. Microbiol.* 55(6), 1457-1465.

Blanchette, R. A., Krueger, E. W., Haight, J. E., Akhtar, M., and Akin, D. E. (1997). "Cell wall alterations in loblolly pine wood decayed by the white-rot fungus, *Ceriporiopsis subvermispora*," *J. Biotechnol.* 53(2-3), 203-213. DOI: 10.1016/S0168-1656(97)01674-X

Blanchette, R. A., Obst, J. R., and Timell, T. E. (1994). "Biodegradation of compression wood and tension wood by white and brown rot fungi," *Holzforschung* 48(Suppl.), 34-42. DOI: 10.1515/hfsg.1994.48.s1.34

Bland, D. E., Foster, R. C., and Logan, A. F. (1971). "The mechanism of permanganate and osmium tetroxide fixation and the distribution of lignin in the cell wall of *Pinus radiata*," *Holzforschung* 25(5), 137-143. DOI: 10.1515/hfsg.1971.25.5.137

Borgin, K., Parameswaran, N., and Liese, W. (1975). "The effect of aging on the ultrastructure of wood," *Wood Sci. Technol.* 9(2), 87-98. DOI: 10.1007/BF00353388

Brändström, J., Bardage, S. L., Daniel, G., and Nilsson, T. (2003). "The structural organization of the S1 cell wall layer of Norway spruce tracheids," *IAWA J.* 24(1), 27-40. DOI: 10.1163/22941932-90000318

Bucur, V. (2003). "Techniques for high resolution imaging of wood structure: A review," *Meas. Sci. Technol.* 14(12), R91-R98. DOI: 10.1088/0957-0233/14/12/R01

Burgert, I., Frühmann, K., Keckes, J., Fratzl, P., and Stanzl-Tschegg, S. (2004). "Structure–function relationships of four compression wood types: Micromechanical properties at the tissue and fibre level," *Trees* 18(4), 480-485. DOI: 10.1007/s00468-004-0334-y

Burgert, I., and Keplinger, T. (2013). "Plant micro- and nanomechanics: experimental techniques for plant cell-wall analysis," *J. Exp. Bot.* 64(15), 4617-4633. DOI: 10.1093/jxb/ert255

Capco, D. G., Krochmalnic, G., and Penman, S. (1984). "A new method of preparing embeddment-free sections for transmission electron microscopy: Applications to the cytoskeletal framework and other three-dimensional networks," *J. Cell Biol.* 98(5), 1879-1885. DOI:10.1083/jcb.98.5.1878

Chafe, S. C. (1974). "On the lamellate structure of the S2 layer," *Protoplasma* 79(1-2), 145-158. DOI: 10.1007/BF02055786

Ciesielski, P. N., Matthews, J. F., Tucker, M. P., Beckham, G. T., Crowley, M. F., Himmel, M. E., and Donohoe, B. S. (2013). "Microfibrils, 3D electron tomography of pretreated biomass informs atomic modeling of cellulose," *ACS Nano.* 7(9), 8011-8019. DOI: 10.1021/nn4031542

Côté, W. A. Jr. (1964). *Cellular Ultrastructure of Woody Plants*, Syracuse University Press, New York.

Côté, W. A. (1967). *Wood Ultrastructure: An Atlas of Electron Micrographs*, University of Washington Press.

Côté, W. A. (1981). "Ultrastructure-Critical domain for wood behavior," *Wood Sci. Technol.* 15(1), 1-29. DOI: 10.1007/BF00366498

Côté, W. A. Jr., Day, A. C., Kutscha, N. P., and Timell, T. E. (1967). "Studies on compression wood. V. Nature of the compression wood formed in the early springwood of conifers," *Holzforschung* 21(6), 180-186. DOI: 10.1515/hfsg.1967.21.6.180

Côté, W. A. Jr., Day, A. C., and Timell, T. E. (1969). "A contribution to the ultrastructure of tension wood fibers," *Wood Sci. Technol.* 3(4), 257-271. DOI: 10.1007/BF00352301

Côté, W. A., Koran, Z., and Day, A. C. (1964). "Replica techniques for electron microscopy of wood and paper," *TAPPI J.* 47(8), 477.

Dadswell, H. E., and Wardrop, A. B. (1955). "The structure and properties of tension wood," *Holzforschung* 9(4), 97-104. DOI: 10.1515/hfsg.1955.9.4.97

Daniel, G. (1994). "Use of electron microscopy for aiding our understanding of wood biodegradation," *FEMS Microbiol. Rev.* 13(2-3), 199-233. DOI: 10.1111/j.1574-6976.1994.tb00043.x

Daniel, G. (2007). *Ljungberg Textbook: Pulp and Paper Chemistry and Technology (Book 1)*, M. Ek, G. Gellerstedt and G. Henriksson (eds.), KTH, Stockholm.

Daniel, G., Goodell, B., Jellison, J., Paszczynski, A., and Crawford, R. (1991). "Use of monoclonal antibodies to detect Mn (II)-peroxidase in birch wood degraded by *Phanerochaete chrysosporium*," *Appl. Microbiol. Biotechnol.* 35(5), 674-680. DOI: 10.1007/BF00169636

Daniel, G., Pettersson, B., Nilsson, T., and Volc, J. (1990). "Use of immunogold cytochemistry to detect Mn(II)-dependent and lignin peroxidases in wood degraded by the white-rot fungi *Phanerochaete chrysosporium* and *Lentinula edodes*," *Can. J. Bot.* 68(4), 920-933. DOI: 10.1139/b90-118

Daniel, G., Volc, J., and Niku-Paavola, M. L. (2004). "Cryo-FE-SEM & TEM immuno-techniques reveal new details for understanding white-rot decay of lignocellulose," *C. R. Biol.* 327(9-10), 861-871. DOI: 10.1016/j.crvi.2004.08.003

De Carlo, S., and Harris, J. R. (2011). "Negative staining and cryo-negative staining of macromolecules and viruses for TEM," *Micron* 42(2), 117-131. DOI: 10.1016/j.micron.2010.06.003

de Lhoneux, B., Antoine, R., and Côté, W. A. (1984). "Ultrastructure implications of gamma-irradiation of wood," *Wood Sci. Technol.* 18(3), 161-176. DOI: 10.1007/BF00367531

Ding, S. U., and Himmel, M. E. (2006). "The maize primary cell wall microfibril: A new model derived from direct visualization," *J. Agric. Food Chem.* 54(3), 597-606. DOI: 10.1021/jf051851z

Donaldson, L. A. (1992). "Lignin distribution during latewood formation in *Pinus radiata* D. Don," *IAWA J.* 13(4), 381-387. DOI: 10.1163/22941932-90001291

bioresources.com

Donaldson, L. A. (1997). "Ultrastructure of transwall fracture surfaces in radiata pine wood using transmission electron microscopy and digital image processing," *Holzforschung* 51(4), 303-308. DOI: 10.1515/hfsg.1997.51.4.303,

Donaldson, L. A. (2001). "Lignification and lignin topochemistry – an ultrastructural view," *Phytochem.* 57(6), 859-873. DOI: 10.1016/S0031-9422(01)00049-8

Donaldson, L. A. (2002). "Abnormal lignin distribution in wood from severely drought stressed *Pinus radiata* trees," *IAWA J.* 23(2), 161-178. DOI: 10.1163/22941932-90000295

Donaldson, L. A., and Singh, A. P. (1998). "Bridge-like structure between cellulose microfibrils in radiata pine (*Pinus radiata* D.Don) kraft pulp and holocellulose," *Holzforschung* 52(5), 449-454. DOI: 10.1515/hfsg.1998.52.5.449

Donaldson, L. A. and Xu, P. (2005). "Microfibril orientation across the secondary cell wall of radiata pine tracheids," *Trees* 19(6), 644-653. DOI: 10.1007/s00468-005-0428-1

Duchesne, I., and Daniel, G. (1999). "The ultrastructure of wood fibre surfaces as shown by a variety of microscopical methods - A review," *Nord. Pulp. Pap. Res. J.* 14(2), 129-139. DOI: 10.3183/NPPRJ-1999-14-02-p129-139

Duchesne, I., Takabe, K., and Daniel, G. (2003). "Ultrastructural localisation of glucomannan in kraft pulp fibres," *Holzforschung* 57(1), 62-68. DOI: 10.1515/HF.2003.010

Dünisch, O., Bauch, J., Müller, M., and Greis, O. (1998). "Subcellular quantitative determination of K and Ca in phloem, cambium, and xylem cells of spruce (*Picea abies* [L.] Karst.) during earlywood and latewood formation," *Holzforschung* 52(6), 582-588. DOI: 10.1515/hfsg.1998.52.6.582

Eder, M., Arnould, O., Dunlop, J. W. C., Hornatowska, J., Salmén, L. (2013). "Experimental micromechanical characterization of wood cell walls," *Wood Sci. Technol.* 47(1), 163-182. DOI: 10.1007/s00226-012-0515-6

Emerton, H. W., and Goldsmith, V. (1956). "The structure of the outer secondary wall of pine tracheids from kraft pulps," *Holzforschung* 10(4), 108-115. DOI:

Emons, A. M., and Mulder, B. M. (2000). "How the deposition of cellulose microfibrils builds cell wall architecture," *Trends Plant Sci.* 5(1), 35-40. DOI: 10.1016/S1360-1385(99)01507-1

Eriksson, I., Lidbrandt, O., and Westermark, U. (1988). "Lignin distribution in birch (*Betula verrucosa*) as determined by mercurization with SEM- and TEM-EDXA," *Wood Sci. Technol.* 22(3), 251-257. DOI: 10.1007/BF00386020

Fahlén, J., and Salmén, L. (2005). "Pore and matrix distribution in the fiber wall revealed by Atomic force microscopy and image analysis," *Biomacromol.* 6(1), 433-438. DOI: 10.1021/bm040068x

Farber, J., Lichtenegger, H. C., Reiterer, A., Stanzl-Tschegg, S., and Fratzl, P. (2001). "Cellulose microfibril angles in a spruce branch and mechanical implications," *J. Mater. Sci.* 36(21), 5087-5092. DOI: 10.1023/A:1012465005607

Fernandes, A. N., Thomas, L. H., Altaner, C. M., Callow, P., Forsyth, V. T., Apperley, D. C., Kennedy, C. J., and Jarvis, M. C. (2011). "Nanostructure of cellulose microfibrils in spruce wood," *Proc. Natl. Acad. Sci.* 108(47), E1195-E1203. DOI: 10.1073/pnas.1108942108

Fernando, D., and Daniel, G. (2008). "Exploring Scots pine fibre development mechanisms during TMP processing: Impact of cell wall ultrastructure

(morphological and topochemical) on negative behavior," *Holzforschung* 62(5), 597-607. DOI: 10.1515/HF.2008.089

Fosiner, R., Messner, K., Stachelberger, H., and Röhr, M. (1985). "Wood decay by basidiomycetes: Extracellular tripartite membranous structures," *Trans. Br. Mycol. Soc.* 85(2), 257-266. DOI: 10.1016/S0007-1536(85)80187-X

Frank, J. (2006). *Three-Dimensional Electron Microscopy of Macromolecular Assemblies: Visualization of Biological Molecules in Their Native State*, Oxford University Press, Oxford, New York. DOI: 10.1093/acprof:oso/9780195182187.001.0001

Frey-Wyssling, A., and Mühlethaler, K. (1963). "Die Elementarfibrillen der Cellulose," *Die Makromolekulare Chemie* 62(1), 25-30. DOI: 10.1002/macp.1963.020620103

Fromm, J., Rockel, B., Lautner, S., Windeisen, E., and Wanner, G. (2003). "Lignin distribution in wood cell walls determined by TEM and backscattered SEM techniques," *J. Struct. Biol.* 143(1), 77-84. DOI: 10.1016/S1047-8477(03)00119-9

Fukushima, K., and Terashima, N. (1991). "Heterogeneity in formation of lignin. Part XV: Formation and structure of lignin in compression wood of *Pinus thunbergii* studied by microautoradiography," *Wood Sci. Technol.* 25(5), 371-381. DOI: 10.1007/BF00226177

Gao, J., Kim, J.S., Terziev, N., Allegretti, O., and Daniel, G. (2014). "Chemical and ultrastructural changes in compound middle lamella (CML) regions of softwoods thermally modified by the Termovuoto process," *Holzforschung* 68(7), 849-859. DOI: 10.1515/hf-2013-0221

Gierlinger, N., Keplinger, T., and Harrington, M. (2012). "Imaging of plant cell walls by confocal Raman microscopy," *Nat. Protoc.* 7(9), 1694-1708. DOI: 10.1038/nprot.2012.092

Gierlinger, N., Luss, S., König, C., Konnerth, J., Eder, M., and Fratzl, P. (2010). "Cellulose microfibril orientation of *Picea abies* and its variability at the micron-level determined by Raman imaging," *J. Exp. Bot.* 61(2), 587-595. DOI: 10.1093/jxb/erp325

Goodell, B., Jellison, J., Liu, J., Daniel, G., Paszczynski, A., Fekete, F., Krishnamurthy, S., Jun, L., and Xu, G. (1997). "Low molecular weight chelators and phenolic compounds isolated from wood decay fungi and their role in the fungal biodegradation of wood," *J. Biotechnol.* 53(2-3), 133-162. DOI: 10.1016/S0168-1656(97)01681-7

Greyer, G. (1973). *Ultrahistochemie*, Gustav Fischer VEB, Stuttgart, Germany.

Hafrén, J., Fujino, T., Itoh, T., Westermark, U., and Terashima, N. (2000). "Ultrastructural changes in the compound middle lamella of *Pinus thunbergii* during lignification and lignin removal," *Holzforschung* 54(3), 234-240. DOI: 10.1515/HF.2000.040

Hafrén, J., and Westermark, U. (2001). "Distribution of acidic and esterified polygalacturonans in sapwood of spruce, birch and aspen," *Nordic Pulp. Pap. Res. J.* 16(4), 284-290. DOI: 10.3183/NPPRJ-2001-16-04-p284-290

Harada, H. (1965). "Ultrastructure and organization of gymnosperm cell walls," W. A. Côté Jr. (ed.), *Cellular Ultrastructure of Woody plants*, Syracuse University Press, Syracuse, New York, pp. 215-233.

Hayat, M. A. (2002). *Microscopy, Immunohistochemistry, and Antigen Retrieval Methods for Light and Electron Microscopy*, Kluwer Academic Publishers, Hingham, MA. DOI: 10.1007/b112626

Hepler, P. K., and Newcombe, E. H. (1963). "The fine structure of young tracheary elements arising by redifferentiation of parenchyma in wounded *Coleus* stem," *J. Expl. Bot.* 14(3), 496-503. DOI: 10.1093/jxb/14.3.496

Highley, T. L., Murmanis, L., and Palmer, J. G. (1983). "Electron microscopy of cellulose decomposition by brown-rot fungi," *Holzforschung* 37(6), 271-277. DOI: 10.1515/hfsg.1983.37.6.271

Hodge, A. J., and Wardrop, A. B. (1950). "An electron-microscopic investigation of the cell-wall organization of conifer tracheids," *Nature* 165(1490), 272-273. DOI: 10.1038/165272a0

Hult, E. L., Iversen, T., and Sugiyama, J. (2003). "Characterization of the supermolecular structure of cellulose in wood pulp fibers," *Cellulose* 10(2), 103-110. DOI: 10.1023/A:1024080700873

Hänninen, T., Kontturi, E., and Vuorinen, T. (2011). "Distribution of lignin and its coniferyl alcohol and coniferyl aldehyde groups in *Picea abies* and *Pinus sylvestris* as observed by Raman imaging," *Phytochem.* 72(14-15), 1889-1895. DOI: 10.1016/j.phytochem.2011.05.005

Jiang, H., Ruokolainen, J., Young, N., Oikawa, T., Nasibulin, A. G., Kirkland, A., and Kauppinen, E. I. (2012). "Performance and early applications of a versatile double aberration-corrected JEOL-2200FS FEG TEM/STEM at Aalto University," *Micron* 43(4), 545-550. DOI: 10.1016/j.micron.2011.10.004

Joseleau, J. P., Imai, T., Kuroda, K., and Ruel, K. (2004). "Detection in situ and characterization of lignin in the G-layer of tension wood fibres of *Populus deltoids*," *Planta* 219(2), 338-345. DOI: 10.1007/s00425-004-1226-5

Joseleau, J. P., and Ruel, K. (1997). "Study of lignification by non invasive techniques in growing maize internodes – An investigation by Fourier transform infrared, cross-polarisation-magic angle spinning 13C-nuclear magnetic resonance spectroscopy," *Plant Physiol.* 114(3), 1123-1133. DOI: 10.1104/pp.114.3.1123

Kallavus, U., and Gravitis, J. (1995). "A comparative investigation of the ultrastructure of steam exploded wood with light, scanning and transmission electron microscopy," *Holzforschung* 49(2), 182-188. DOI: 10.1515/hfsg.1995.49.2.182

Kerr, A. J., and Goring, D. A. I. (1975). "Ultrastructural arrangement of the wood cell wall," *Cellul. Chem. Technol.* 9(6), 563-573.

Khalil, H. S. A., Alwani, M. S., and Omar, A. K. M. (2006). "Chemical composition, anatomy, lignin distribution, and cell wall structure of Malaysian plant waste fibers," *BioResources* 1(2), 220-232. DOI: 10.15376/biores.1.2.220-232

Khalili, S., Daniel, G., and Nilsson, T. (2000). "Use of soft rot fungi for studies on the microstructure of kapok (*Ceiba pentandra* (L.) Gaertn.) fibre cell walls," *Holzforschung* 54(3), 229-233. DOI: 10.1515/HF.2000.039

Khalil, H. S. A., Yusra, A. F. I., Bhat, A. H., and Jawaid, M. (2010). "Cell wall ultrastructure, anatomy, lignin distribution, and chemical composition of Malayasian cultivated kenaf fiber," *Ind. Crops Prod.* 31(1), 113-121. DOI: doi:10.1016/j.indcrop.2009.09.008

Khristova, P., Bentcheva, S., and Karar, I. (1998). "Soda-AQ pulp blends from kenaf and sunflower stalks," *Biores. Technol.* 66(2), 99-103. DOI: 10.1016/S0960-8524(98)00058-3

Kim, J. S., Awano, T., Yoshinaga, A., and Takabe, K. (2010a). "Immunolocalization and structural variations of xylan in differentiating earlywood tracheid cell walls of *Cryptomeria japonica*," *Planta* 232(4), 817–824, DOI: 10.1007/s00425-010-1225-7

Kim, J. S., Awano, T., Yoshinaga, A., and Takabe, K. (2010b). "Temporal and spatial immunolocalization of glucomannans in differentiating earlywood tracheid cell walls of *Cryptomeria japonica*," *Planta* 232(2), 545-554. DOI: 10.1007/s00425-010-1189-7

Kim, J. S., Awano, T., Yoshinaga, A., and Takabe, K. (2011). "Occurrence of xylan and mannan polysaccharides and their spatial relationship with other cell wall components in differentiation compression wood tracheids of *Cryptomeria japonica*," *Planta* 233(4), 721-735. DOI: 10.1007/s00425-010-1333-4

Kim, Y. S., Choi, J. H., and Bae, H. J. (1992). "Ultrastructural localization of extracellular fungal metabolites from *Tyromyces palustris* using TEM (transmission electron microscopy) and immunogold labeling," *Mokuzai Gakkaishi* 38(5), 490-494.

Kim, Y. S., Goodell, B., and Jellison, J. (1993). "Immunogold labeling of extracellular metabolites from the white-rot fungus *Trametes versicolor*," *Holzforschung* 47(1), 25-28. DOI: 10.1515/hfsg.1993.47.1.25

Kim, Y. S., Lee, K. H., Kim, J. K., and Singh, A. P. (2014). "Lignin masks the presence of fibrillar network structure in the cell corner middle lamella (CCML)," *Holzforschung* 69(1), 121-126. DOI: 10.1515/hf-2014-0032

Kim, Y. S., and Singh, A. P. (1999). "Micromorphological characteristics of compression wood degradation in waterlogged archeological pine wood," *Holzforschung* 53(4), 381-385. DOI: 10.1515/HF.1999.063

Koch, G., and Schmitt, U. (2013). *Cellular Aspects of Wood Formation*, J. Fromm (ed.), Springer, New York.

Krässig, H. A. (1993). *Cellulose - Structure, Accessibility and Reactivity*, Gordon and Breach Science Publishers, Yverdon, Switzerland.

Kukkola, E. M., Koutaniemi, S., Gustafsson, M., Karhunen, P., Ruel, K., Lundell, T. K., Saranpää, P., Brunow, G., Teeri, T. H., and Fagerstedt, T. V. (2003). "Localization of dibenzodioxocin substructures in lignifying Norway spruce xylem by transmission electron microscopy-immunogold labeling," *Planta* 217(2), 229-237. DOI: 10.1007/s00425-003-0983-x

Kuo, J. (2007). *Electron Microscopy: Methods and Protocols*, Humana Press Inc., New Jersey, USA.

Lautner, S., Zollfrank, C., and Fromm, J. (2012). "Microfibril angle distribution of poplar tension wood," *IAWA J.* 33(4), 431-439. DOI: 10.1163/22941932-90000105

Lehringer, C., Daniel, G., and Schmitt, U. (2009) TEM/FE-SEM studies on tension wood fibres of *Acer* spp., *Fagus sylvatica* L. and *Quercus robur* L.," *Wood Sci. Technol.* 43(7-8), 691-702. DOI: 10.1007/s00226-009-0260-7

Lei, X., Zhao, Y., Li, K., and Pelletier, A. (2012). "Improved surface properties of CTMP fibers with enzymatic pretreatment of wood chips prior to refining," *Cellulose* 19(6), 2205-2215. DOI: 10.1007/s10570-012-9792-3

Lequart, C., Ruel, K., Lapierre, C., Pollet, B., and Kurek, B. (2000). "Abiotic and enzymatic degradation of wheat straw cell wall: A biochemical and ultrastructural investigation," *J. Biotechnol.* 80(3), 249-259. DOI: 10.1016/S0168-1656(00)00267-4

Lichtenegger, H., Muller, M., Paris, O., Riekel, C., and Fratzl, P. (1999). "Imaging of the helical arrangement of cellulose fibrils in wood by synchrotron X-ray microdiffraction," *J. Appl. Crystallogr.* 32(6), 1127-1133. DOI: 10.1107/S0021889899010961

Manley, R. S. J. (1964). "Fine structure of native cellulose microfibrils," *Nature* 204(4964), 1155-1157. DOI: 10.1038/2041155a0

Marchetti, V., Ghanbaja, P., and Loubinoux, B. (2000). "Localization and characterization by TEM and EELS of manganese species during graft copolymerization of acrylic acid onto sawdust using $KMnO_4$ as initiator," *Holzforschung* 54(5), 553-556. DOI: 10.1515/HF.2000.093

Maurer, A., and Fengel, D. (1990). "A new process for improving the quality and lignin staining of ultrathin sections from wood tissues," *Holzforschung* 44(6), 453-460. DOI: 10.1515/hfsg.1990.44.6.453

Maurer, A., and Fengel, D. (1991). "Electron microscopic representation of structural details in softwood cell walls by very thin ultramicrotome sections," *Holz Roh-Werkstoff* 49(2), 53-56. DOI: 10.1007/BF02662800

Ma, J. F., Yang, G. H., Mao, J. Z., and Xu, F. (2011b). "Characterization of anatomy, ultrastructure and lignin microdistribution in *Forsythia suspensa*," *Ind. Crops Prod.* 33(2), 358-363. DOI: 10.1016/j.indcrop.2010.11.009

Ma, J., Zhang, Z., Yang, G., Mao, J., and Xu, F. (2011a). "Ultrastructural topochemistry of cell wall polymers in *Populus nigra* by transmission electron microscopy and Raman imaging," *BioResources* 6(4), 3944-3959. DOI:

Michler, G.H. (2008). *Electron Microscopy of Polymers*, Springer-Verlag, Berlin, Germany. DOI: 10.1007/978-3-540-36352-1

Molin, U., and Daniel, G. (2004). "Effects of refining on the fiber structure of kraft pulps as revealed by FE-SEM and TEM: Influence of alkaline degradation," *Holzforschung* 58(3), 226-232. DOI: 10.1515/HF.2004.035

Mueller, S. C., and Brown, J. R. M. (1980). "Evidence for an intramembrane component associated with a cellulose microfibril-synthesizing complex in higher plants," *J. Cell Biol.* 84(2), 315-326. DOI: 10.1083/jcb.84.2.315

Mühlethaler, K. (1949). "Electron micrographs of plant fibers," *Biochim. Biophys. Acta* 3(), 15-25. DOI: 10.1016/0006-3002(49)90075-X

Mühlethaler, M. (1969). "Fine structure of natural polysaccharide systems," *J. Polym. Sci.*. 28(1), 305-316. DOI: 10.1002/polc.5070280124

Nicole, M., Chamberland, H., Geiger, J. P., Lecours, N., Valero, J., Rio, B., and Ouellette, G. B. (1992). "Immunocytochemical localization of laccase L1 in wood decayed by *Rigidoporus lignosus*," *Appl. Environ. Microbiol.* 58(5), 1727-1739.

Nishiyama, Y., Langan, P., and Chanzy, H. (2002). "Crystal structure and hydrogen-bonding system in cellulose Iβ from synchrotron x-ray and neutron fiber diffraction," *J. Am. Chem. Soc.* 124(31), 9074-9082. DOI: 10.1021/ja0257319

Norberg, P. H., and Meier, H. (1966). "Physical and chemical properties of the gelatinous layer in tension wood fibers of aspen (*Populus tremula* L.)," *Holzforschung* 20(6), 174-178. DOI: 10.1515/hfsg.1966.20.6.174

Northcote, D. H., and Lamport, D. T. A. (1960). "Hydroxyproline in primary walls of higher plants," *Nature* 188(4751), 665-666. DOI: 10.1038/188665b0

O'Sullivan, A. C. (1997). "Cellulose: The structure slowly unravels," *Cellulose* 4(3), 173-207. DOI: 10.1023/A:1018431705579

Paszczynski, A., Blanchette, R. L., and Crawford, R. A. (1988). "Delignification of wood chips and pulps by using natural and synthetic porphyrins: Models of fungal decay,"*Appl. Environ. Microbiol.*54(1), 62-68.

Pedersen, N. B., Schmitt, U., Koch, G., Felby, C., and Thygesen, L. G. (2014). "Lignin distribution in waterlogged archaeological *Picea abies* (L.) Karst degraded by erosion bacteria," *Holzforschung* 68(7), 791-798. DOI: 10.1515/hf-2013-0228

bioresources.com

Peura, M., Müller, M., Vainio, U., Sarén, M. P., Saranpää, P., and Serimaa, R. (2008). "X-ray microdiffraction reveals the orientation of cellulose microfibrils and the size of cellulose crystallites in single Norway spruce tracheids," *Trees* 22(1), 49-61. DOI: 10.1007/s00468-007-0168-5

Pilate, G., Chabbert, B., Cathala, B., Yoshinaga, A., Leplé, J. C., Laurans, F., Lapierre, C., and Ruel, K. (2004). "Lignification and tension wood," *C. R. Biol.* 327(9-10), 889-901. DOI: 10.1016/j.crvi.2004.07.006

Preston, R. D., Nicolai, E., Reed, R., and Millard, A. (1948). "An electron microscope study of cellulose in the wall of *Valonia ventricosa*," *Nature* 162, 665-667. DOI: 10.1038/162665a0

Preston, R. D., and Ripley, G. W. (1954). "Electron diffraction diagrams of cellulose micro-fibrils in *Valonia*," *Nature* 174, 76-77. DOI:10.1038/174076a0

Prislan, P., Koch, G., Cufar, K., Gricar, J., and Schmitt, U. (2009). "Topochemical investigations of cell walls in developing xylem of beech (*Fagus sylvatica* L.)," *Holzforschung* 63(4), 482-490. DOI: 10.1515/HF.2009.079

Prodhan, A. K. M. A., Ohtani, J., Funada, R., Abe, H., and Fukazawa, K. (1995). "Ultrastructural investigation of tension wood fiber in *Fraxinus mandshurica* Rupr. var. japonica Maxim," *Ann. Bot.* 75(3), 311-317. DOI: 10.1006/anbo.1995.1026

Raghavan, R., Adusumalli, R. B., Buerki, G., Hansen, S., Zimmermann, T., and Michler, J. (2012). "Deformation of the compound middle lamella in spruce latewood by micro-pillar compression of double cell walls," *J. Mater. Sci.* 47(16), 6125-6130. DOI: 10.1007/s10853-012-6531-y

Rapp, A. O., Bestgen, H., Adam, W., and Peek, R. D. (1999). "Electron energy loss spectroscopy (EELS) for quantification of cell-wall penetration of a melamine resin," *Holzforschung* 53(2), 111-117. DOI: 10.1515/HF.1999.018

Rehbein, M., Koch, G., Schmitt, U., and Huckfeldt, T. (2013). "Topochemical and transmission electron microscopic studies of bacterial decay in pine (*Pinus sylvestris* L.) harbor foundation piles," *Micron* 44, 150-158. DOI: 10.1016/j.micron.2012.05.012

Revol, J.-F. (1985). "Change of the *d* spacing in cellulose crystals during lattice imaging," *J. Mater.Sci. Lett.* 4(11), 1347-1349. DOI: 10.1007/BF00720097

Reza, M., Rojas, L. G., Kontturi, E., Vuorinen, T., and Ruokolainen, J. (2014a). "Accessibility of cell wall lignin in solvent extraction of ultrathin spruce wood sections," *ACS Sustainable Chem. Eng.* 2(4), 804-808. DOI: 10.1021/sc400470m

Reza, M., Ruokolainen, J., and Vuorinen, T. (2014b). "Out-of-plane orientation of cellulose elementary fibrils on spruce tracheid wall based on imaging with high-resolution transmission electron microscopy," *Planta* 240(3), 565-573. DOI: 10.1007/s00425-014-2107-1

Roelofsen, P. A. (1959). *The Plant Cell Wall*, Borntraeger, Berlin, Germany. DOI: 10.1016/0003-9861(61)90372-1

Ruel, K., Burlat, V., and Joseleau, J. P. (1999). "Relationship between ultrastructural topochemistry of lignin and wood properties," *IAWA J.* 20(2), 203-211. DOI: 10.1163/22941932-90000681

Ruel, K., Nishiyama, Y., and Joseleau, J. P. (2012). "Crystalline and amorphous cellulose in the secondary walls of Arabidopsis," *Plant Sci.* 193, 48-61. DOI: 0.1016/j.plantsci.2012.05.008

Ruska, E. (1934). "Uber Fortschritte im Bau und in der Leistung des magnetischen Elektronenmikroskops (On the progress in the construction and performance of the

---

bioresources.com

magnetic electron microscope),” *Z. Phys.* 87(9-10), 580-602. DOI: 10.1007/BF01333326

Råberg, U., and Daniel, G. (2009). “Brown rot decay of copper-chromated-phosphorus impregnated fence poles: Characterization by molecular analysis and microscopy,” *Int. Biodeterior. Biodegrad.* 63(7), 906-912. DOI: doi:10.1016/j.ibiod.2009.04.009

Saito, T., Nishiyama, Y., Putaux, J. L., Vignon, M., and Isogai, A. (2006). “Homogeneous suspensions of individualized microfibrils from TEMPO-catalyzed oxidation of native cellulose,” *Biomacromol.* 7(6), 1687-1691. DOI: 10.1021/bm060154s

Saka, S., and Goring, D. A. I. (1988). “The distribution of lignin in white birch wood as determined by bromination with TEM-EDXA,” *Holzforschung* 42(3), 149-153. DOI: 10.1515/hfsg.1988.42.3.149

Sandquist, D., Filonova, L., von Schantz, L., Ohlin, M., and Daniel, G. (2010). “Microdistribution of xyloglucan in differentiating poplar cells,” *BioResources* 5(2), 796-807. DOI: 10.15376/biores.5.2.796-807

Sawyer, L. C., Grubb, D. T., and Meyers, G. F. (2008). *Polymer Microscopy*, 3rd Edition, Springer, New York.

Saxe, F., Eder, M., Benecke, G., Aichmayer, B., Fratzl, P., Burgert, I., and Rüggeberg, M. (2014). “Measuring the distribution of cellulose microfibril angles in primary cell walls by small angle X-ray scattering,” *Plant Methods* 10(1), 25-32. DOI: 10.1186/1746-4811-10-25

Scurfield, G. (1973). “Reaction wood: Its structure and function: Lignification may generate the force active in restoring the trunks of leaning trees to the vertical,” *Science* 179(4074), 647-655. DOI: 10.1126/science.179.4074.647

Singh, A. P., and Daniel, G. (2001). “The S2 layer in the tracheid walls of *Picea abies* wood: inhomogeneity in lignin distribution and cell wall microstructure,” *Holzforschung* 55(4), 373-378. DOI: 10.1515/HF.2001.062

Singh, A., Daniel, G., and Niisson, T. (2002a). “Ultrastructure of the S2 layer in relation to lignin distribution in *Pinus radiata* tracheids,” *J. Wood Sci.* 48(2), 95-98. DOI: 10.1007/BF00767284

Singh, A., Daniel, G., and Nilsson, T. (2002b). “High variability in the thickness of the S3 layer in *Pinus radiata* tracheids,” *Holzforschung* 56(2), 111-116. DOI: 10.1515/HF.2002.019

Singh, A. P., Kim, Y. S., Chung, G. C., Park, B. D., and Wong, A. H. H. (2003). “TEM examination of surface characteristics of rubberwood (*Hevea brasiliensis*) HTMP fibers,” *Holzforschung* 57(6), 579-584. DOI: 10.1515/HF.2003.087

Singh, A. P., Sell, J., Schmitt, U., Zimmermann, T., and Dawson, B. (1998). “Radial striation of the S2 layer in mild compression wood tracheids of *Pinus radiata*,” *Holzforschung* 52(6), 563-566. DOI: 10.1515/hfsg.1998.52.6.563

Solala, I., Antikainen, T., Reza, M., Johansson, L. S., Hughes, M., and Vuorinen, T. (2013). “Spruce fiber properties after high-temperature thermomechanical pulping (HT-TMP),” *Holzforschung* 68(2), 195-201. DOI: 10.1515/hf-2013-0083

Spurr, A. R. (1969). “A low viscosity embedding medium for electron microscopy,” *J. Ultrastruct. Res.* 26(1-2), 31-43. DOI: 10.1016/S0022-5320(69)90033-1

Streit, W., and Fengel, F. (1994). “Heartwood formation in *Quebracho colorado* (*Schinopsis balansae* Engl.): Tannin distribution and penetration of extractives into the cell wall,” *Holzforschung* 48(5), 361-367. DOI: 10.1515/hfsg.1994.48.5.361

Studer, D., and Gnaegi, H. (2000). "Minimal compression of ultrathin sections with use of an oscillating diamond knife," *J. Microsc.* 197(1), 94-100. DOI: 10.1046/j.1365-2818.2000.00638.x

Sugiyama, J., Harada, H., Fujiyoshi, Y., and Uyeda, N. (1985). "Lattice images of cellulose microfibrils," *Denshi Kenbikyö* 20, 143-147.

Sugiyama, J., Otsuka, Y. Murase, H., and Harada, H. (1986). "Toward direct imaging of cellulose microfibrils in wood," *Holzforschung* 40(Suppl.), 31-36.

Sugiyama, J., Persson, J., and Chanzy, H. (1991a). "Combined infrared and electron diffraction study of the polymorphism of native celluloses," *Macromol.* 24(9), 2461-2466. DOI: 10.1021/ma00009a050

Sugiyama, J., Vuong, R., and Chanzy, H. (1991b). "Electron diffraction study on the two crystalline phases occurring in native cellulose from an algal cell wall," *Macromol.* 24(14), 4168-4175. DOI: 10.1021/ma00014a033

Terashima, N., and Fukushima, K. (1988). "Heterogeneity in formation of lignin-XI: An autoradiographic study of the heterogeneous formation and structure of pine lignin," *Wood Sci. Technol.* 22(3), 259-270. DOI: 10.1007/BF00386021

Timell, T. E. (1973). "Studies on opposite wood in conifers. Part III: Distribution of lignin," *Wood Sci. Technol.* 7(3), 163-172. DOI: 10.1007/BF00355547

Timell, T. E. (1982). "Recent progress in the chemistry and topochemistry of compression wood," *Wood Sci. Technol.* 16(2), 83-122. DOI: 10.1007/BF00351097

Trtik, P., Dual, J., Keunecke, D., Mannes, D., Niemz, P., Stähli, P., Kaestner, A., Groso, A., and Stampanoni, M. (2007). "3D imaging of microstructure of spruce wood," *J. Struct. Biol.* 159(1), 46-55. DOI: 10.1016/j.jsb.2007.02.003

Wada, M., Okano, T., Sugiyama, J., and Horii, F. (1995). "Characterization of tension and normally lignified wood cellulose in *Populus maximowiczii*," *Cellulose* 2(4), 223-233. DOI: 10.1007/BF00811814

Wallstörm, L., and Lindberg, K. A. H. (2000). "Distribution of added chemicals in the cell walls of high temperature dried and green wood of Swedish pine, *Pinus sylvestries*," *Wood Sci. Technol.* 34(4), 327-336. DOI: 10.1007/s002260000050

Wardrop, A. B. (1954). "The fine structure of the conifer tracheid," *Holzforschung* 8(1), 12-29. DOI: 10.1515/hfsg.1954.8.1.12

Wardrop, A. B. (1957). "The organization and properties of the outer layer of the secondary wall in conifer tracheids," *Holzforschung* 11(4), 102-110. DOI: 10.1515/hfsg.1957.11.4.102

Westermark, U., Lidbrandt, O., and Eriksson, I. (1988). "Lignin distribution in spruce (*Picea abies*) determined by mercurization with SEM-EDXA technique," *Wood Sci. Technol.* 22(3), 243-250. DOI: 10.1007/BF00386019

Williams, D. B., and Carter, C. B. (2009). *Transmission Electron Microscopy: A Textbook for Materials Science*, 2nd Edition, Springer, New York.

Xu, P., Donaldson, L. A., Gergely, Z. R., and Staehelin, L. A. (2007). "Dual-axis electron tomography: a new approach for investigating the spatial organization of wood cellulose microfibrils," *Wood Sci. Technol.* 41(2), 101-116. DOI: 10.1007/s00226-006-0088-3

Xu, F., Sun, R. C., Lu, Q., and Jones, G. L. (2006b). "Comparative study of anatomy and lignin distribution in normal and tension wood of *Salix gordejecii*," *Wood Sci. Technol.* 40(5), 358-370. DOI: 10.1007/s00226-005-0049-2

Xu, F., Zhong, X. C., Sun, R. C., and Lu, Q. (2006a). "Anatomy, ultrastructure and lignin distribution in cell wall of *Caragana Korshinskii*," *Ind. Crops Prod.* 24(2), 186-193. DOI: 10.1016/j.indcrop.2006.04.002

Yoshida, M., Ohta, H., and Okuyama, T. (2002). "Tensile growth stress and lignin distribution in the cell walls of black locust (*Robinia pseudoacacia*)," *J. Wood Sci.* 48(2), 99-105. DOI: 10.1007/BF00767285

Yoshinaga, A., Kusumoto, H., Laurans, F., Pilate, G., and Takabe, K. (2012). "Lignification in poplar tension wood lignified cell wall layers," *Tree Physiol.* 32(9), 1129-1136. DOI: 10.1093/treephys/tps075

Zimmermann, T., and Sell, J. (2003). "Field emission SEM studies on softwood tracheids and hardwood fibres-A review of activities at the EMPA wood laboratory," *Schweiz. Z. Forstwes.* 154(12), 510-515. DOI: 10.3188/szf.2003.0510

Zimmermann, T., Thommen, V., Reimann, P., and Hug, H. J. (2006). "Ultrastructural appearance of embedded and polished wood cell walls as revealed by atomic force microscopy," *J. Struct. Biol.* 156(2), 363-369. DOI: 10.1016/j.jsb.2006.06.007